MINISTÈRE
DE L'ÉDUCATION
NATIONALE

EAD BIO 2

SESSION 2018

AGREGATION
CONCOURS EXTERNE

Section : BIOCHIMIE - GÉNIE BIOLOGIQUE

ÉTUDE DE DOSSIER SCIENTIFIQUE ET TECHNOLOGIQUE

Durée : 4 heures

L'usage du dictionnaire anglais-français est autorisé.
L'usage de tout ouvrage de référence, de tout autre dictionnaire et de tout matériel électronique (y compris la calculatrice) est rigoureusement interdit.

Dans le cas où un(e) candidat(e) repère ce qui lui semble être une erreur d'énoncé, il (elle) le signale très lisiblement sur sa copie, propose la correction et poursuit l'épreuve en conséquence.

De même, si cela vous conduit à formuler une ou plusieurs hypothèses, il vous est demandé de la (ou les) mentionner explicitement.

NB : ***La copie que vous rendrez ne devra, conformément au principe d'anonymat, comporter aucun signe distinctif, tel que nom, signature, origine, etc. Si le travail qui vous est demandé comporte notamment la rédaction d'un projet ou d'une note, vous devrez impérativement vous abstenir de signer ou de l'identifier.***

Tournez la page S.V.P.

L'édition du génome : le système CRISPR-Cas

L'édition du génome, notamment chez les eucaryotes, fait l'objet d'intenses recherches et les différentes techniques développées ouvrent un large champ d'applications.
A l'aide des articles proposés dans le dossier technique et en lien avec le contexte de l'étude, présenter le travail de recherche, tant dans sa dimension scientifique que dans ses aspects technologiques, et ses applications innovantes dans le domaine de la santé. Le candidat veillera également à proposer des mises en perspectives pédagogiques, prolongements des travaux présentés, en lien avec les connaissances générales exigées pour des étudiants de niveau BAC +2. Lors de la composition, l'analyse critique, la maîtrise scientifique et l'esprit de synthèse des candidats seront également appréciés.

Le dossier technique comporte deux parties :

Revue : **A CRISPR CASe for high-throughput silencing**

Jacob Heintze, Christin Luft and Robin Ketteler
Frontiers in Genetics, vol. 4, article 193, October 2013

Publication : **CRISPR-Cpf1 correction of muscular dystrophy mutations in human cardiomyocytes and mice**

Yu Zhang, Chengzu Long, Hui Li, John R. McAnally, Kedryn K. Baskin, John M. Shelton, Rhonda Bassel-Duby, Eric N. Olson
Science Advances, vol. 3, April 2017

INFORMATION AUX CANDIDATS

Vous trouverez ci-après les codes nécessaires vous permettant de compléter les rubriques figurant en en-tête de votre copie.

Ces codes doivent être reportés sur chacune des copies que vous remettrez.

Concours	Section/option	Epreuve	Matière
EAD	7100A	102	7810

frontiers in GENETICS

PERSPECTIVE ARTICLE
published: 07 October 2013
doi: 10.3389/fgene.2013.00193

A CRISPR CASe for high-throughput silencing

Jacob Heintze, Christin Luft and Robin Ketteler*

Medical Research Council Laboratory for Molecular Cell Biology, University College London, London, UK

Edited by:
Rafael E. Carazo Salas, University of Cambridge, UK

Reviewed by:
Neil Hukriede, University of Pittsburgh, USA
Sachin Rustgi, Washington State University, USA
David John Stephens, University of Bristol, UK

***Correspondence:**
Robin Ketteler, Medical Research Council Laboratory for Molecular Cell Biology, University College London, Gower Street, London WC1E 6BT, UK
e-mail: r.ketteler@ucl.ac.uk

Manipulation of gene expression on a genome-wide level is one of the most important systematic tools in the post-genome era. Such manipulations have largely been enabled by expression cloning approaches using sequence-verified cDNA libraries, large-scale RNA interference libraries (shRNA or siRNA) and zinc finger nuclease technologies. More recently, the CRISPR (clustered regularly interspaced short palindromic repeats) and CRISPR-associated (Cas)9-mediated gene editing technology has been described that holds great promise for future use of this technology in genomic manipulation. It was suggested that the CRISPR system has the potential to be used in high-throughput, large-scale loss of function screening. Here we discuss some of the challenges in engineering of CRISPR/Cas genomic libraries and some of the aspects that need to be addressed in order to use this technology on a high-throughput scale.

Keywords: CRISPR, Cas9, RNAi, gene silencing, gene editing, knockdown, screen, high-throughput

BACKGROUND

Advances in lab automation and completion of the human genome project have resulted in the design of large-scale whole-genome libraries encompassing thousands of samples in a single run. These developments build on technological advances made by the pharmaceutical industry that required a need for screening large collections of chemical compounds in a very cost-effective manner and were subsequently adopted by academic institutions for chemical compound screening as well as expression cloning applications. Such large-scale screening approaches have enabled the unbiased identification of cell-based phenotypes and led to several ground-breaking discoveries, in particular for the identification of cell surface and virus receptors (Seed, 1995).

Expression cloning relies on the generation of an expressed cDNA library that can be transfected into target cells for assessment of changes in a cellular reporter activity or phenotype. Over the years, a complementary approach was developed based on the use of "antisense" constructs without a proper understanding of the underlying mechanisms. Eventually, after the discovery of RNA interference in the late 1990s and the development of mammalian siRNA libraries in the early 2000s, such knockdown technologies became mainstream for interrogating gene defects on a genome-wide scale. To date, siRNA genome-wide libraries are still the main application in genomic high-throughput screening, partially because of the lack of alternative methods. In recent years, many key problems of RNAi technology have become apparent, such as off-target effects, variable levels of knockdown efficiency and low-level confidence in hits of screening campaigns (Buehler et al., 2012; Marine et al., 2012). Hence, the siRNA screening community is openly discussing the need for alternative systems to overcome these limitations.

An alternative way of modifying the mammalian genome on a large-scale may lie in the use of genome editing technologies such as the use of targeted endonucleases. While zinc finger nucleases (ZFNs) and transcription activator-like effector nuclease (TALEN)s are highly useful for gene editing, the cost and time to engineer the system makes it incompatible for the generation of large-scale whole-genome libraries. In particular, ZFN or TALENs require engineering of a protein component for each gene locus and this may not be amenable or cost-effective on a large-scale. With the CRISPR (clustered regularly interspaced short palindromic repeats)/Cas9 system, a cost-effective method that combines targeted genome editing with a simple, less time-consuming assay set-up is emerging and may be compatible with high-throughput screening approaches. An overview of the main techniques for genome editing and gene silencing is given in **Table 1** and a detailed assessment of the advantages and disadvantages of genome editing methods has been given elsewhere (Ramalingam et al., 2013).

CRISPR/Cas9

The CRISPR/Cas9 system, originally exploited from *Streptococcus pyogenes*, is a general bacterial host defense mechanism to detect and degrade exogenous sequences from invading bacteriophages (Sorek et al., 2013). Short segments of foreign DNA are processed by CRISPR-associated (Cas) proteins into small elements which are then inserted into the CRISPR locus. RNAs from the CRISPR loci are constitutively transcribed and processed into small RNAs (crRNA) of exogenously derived DNA. These small RNAs then guide other Cas proteins such as Cas9 to mediate sequence-specific degradation of the foreign DNA. As such, the system serves two critical functions of acquired immunity, memory and pathogen elimination, and has some resemblance with acquired immunity in higher organisms. This system relies on the DNA endonuclease Cas9 that is targeted to a specific region of the genome to direct cleavage of the DNA in a sequence-specific manner (Jinek et al., 2012). Binding of Cas9 to the DNA is mediated by a partially complementary *trans*-acting RNA (tracrRNA) and cleavage is directed

Table 1 | Overview of genome editing and gene silencing technologies.

Name	Components	Mechanism of action	Specificity/off-target effects	Possibility to rapidly generate large-scale libraries
Genome editing				
Zinc finger nucleases (ZFNs)	Fok1 restriction nuclease fused to multiple zinc finger peptides; each targeting 3 bp of genomic sequence	Induces double-strand breaks in target DNA	Can have off-target effects	No – requires customization of protein component for each gene
Transcription activator-like effector nucleases (TALENs)	Non-specific DNA-cleaving nuclease fused to a DNA-binding domain specific for a genomic locus	Induces double-strand breaks in target DNA	Highly specific	Feasible, but technically challenging (Reyon et al., 2012)
Homing meganucleases	Endonuclease with a large recognition site for DNA (12–40 base pairs)	Induces double-strand breaks in target DNA	Highly specific	No – limited target sequence specificity available
CRISPR/Cas	20 nt crRNA fused to tracrRNA and Cas9 endonuclease	Induces double-strand breaks in target DNA (wt Cas9) or single-strand DNA nicks (Cas9 nickase)	Some off-target effects that can be minimized by selection of unique crRNA sequences	Yes – requires simple adapter cloning of 20 nt Oligos targeting each gene into a plasmid
Gene silencing				
Post-transcriptional gene silencing (e.g., RNA interference)	Double-stranded RNA	DICER-mediated mRNA degradation; (post-transcriptional)	Can have significant off-target effects	Yes (Moffat et al., 2006)
Morpholino oligonucleotides	Synthetic oligonucleotide analogs	Sterical blocking of translation initiation complex; (post-transcriptional)	Can have significant off-target effects	Feasible, but technically challenging
CRISPRi	sgRNA and catalytically inactive Cas9	Transcriptional repression of RNA synthesis	To be determined	Yes

by a mature CRISPR RNA (crRNA; Deltcheva et al., 2011; Jinek et al., 2012). These three components, the Cas endonuclease, the tracrRNA, and crRNA are the basic constituents of this genome editing system.

By modifying these basic constituents for the use in other organisms, the CRISPR/Cas9 system has been shown to be a useful tool for gene editing and silencing. CRISPR sequences can be engineered which give rise to crRNA directed against specific endogenous genes in various organisms. Significant advances for the use of this technique have been promoted by the generation of a "single-guide RNA" (sgRNA) that combines the function of the tracrRNA and crRNA in a chimeric molecule (Jinek et al., 2012, 2013). By now the CRISPR/Cas9 system has been successfully used to target genomic loci in mammalian cell lines (Cho et al., 2013; Cong et al., 2013; Mali et al., 2013; Wang et al., 2013), zebrafish (Chang et al., 2013; Hwang et al., 2013), fungi (Dicarlo et al., 2013), bacteria (Jiang et al., 2013; Mali et al., 2013), *C. elegans* (Friedland et al., 2013), *Drosophila* (Gratz et al., 2013), plants (Li et al., 2013b; Nekrasov et al., 2013; Shan et al., 2013), rats (Li et al., 2013a,c), and mice (Wang et al., 2013). For instance, gene knockout mice can be rapidly generated when the desired gene locus is targeted via CRISPR/Cas9 (Wang et al., 2013). Quite importantly, multiple loci can be targeted at the same time by incorporation of multiple crRNA sequences (Cho et al., 2013; Wang et al., 2013). In zebrafish, where RNAi-based methods have limited capability, the use of CRISPR has enabled the generation of whole animals deficient in multiple gene loci (Chang et al., 2013; Hwang et al., 2013). The same system has been used to site-specifically insert mloxP sites, making it a novel reverse genetic tool for genome modification (Chang et al., 2013). In zebrafish and *Drosophila* it has been shown that CRISPR/Cas9 genome editing is inheritable with germline transmission reaching nearly 100% (Basset et al., 2013; Hwang et al., 2013; Yu et al., 2013).

Up to date three different versions of the Cas9 component have been described for the use in mammalian cells.

(A) Wild-type humanized (h)Cas9: Wild-type Cas9 will introduce a double-strand break (DSB) at the region it is targeted to, thus resulting in activation of the DSB repair machinery. Consequently, this will lead to insertion or deletion of nucleotides

at the site of injury of the DSB and lead to alterations in the DNA sequence and ultimately in gene expression.

(B) hCas9 D10A nickase: The wild-type endonuclease activity of Cas9 may, however, result in genome rearrangements that can lead to deleterious effects, e.g., selection against cells expressing wild-type Cas9 was observed (Qi et al., 2013). Furthermore, the generation of insertion/deletions (indels) at the target region as a consequence of DSB repair may lead to unwanted side-effects (Ketteler, 2012). To avoid those effects, Cong et al. used a mutant Cas9 nickase that only generates a nick in the genomic DNA at the target region, which in turn is repaired through high-fidelity homology-directed repair, rather than the error-prone Cas9 endonuclease-mediated non-homologous end-joining repair (Cong et al., 2013). The experiments to date suggest that this mutant Cas9 nickase shows similar targeting efficiencies compared to wild-type Cas9. Another advantage of the nickase system is that it can be used for generating knockout as well as knockin genotypes. This can be achieved by co-transfection of a recombination cassette with 5′- and 3′-flanking homology regions. However, knockout/knockin constructs based on the Cas9 nickase system require engineering of homologous recombination cassettes for each gene locus, thus making it technically challenging to implement on a large-scale.

(C) Catalytically dead dCas9: Qi et al. (2013) took a step further to generate a catalytically dead Cas9 lacking endonuclease activity. This resulted in gene silencing rather than gene editing of the target locus. This offers a significant advantage over classic RNAi-based silencing since mRNA synthesis is altered at an early stage of transcription by blocking RNA polymerase and transcript elongation whereas in RNA interference, the expressed synthesized mRNA is degraded. With this novel system, termed CRISPRi, the promoter region can also be targeted to efficiently knock down expression of the transcript. Moreover, Qi et al. (2013) showed that CRISPRi can be used to simultaneously repress multiple target genes (similar to chimeric hairpin constructs in RNAi, Gil-Humanes et al., 2010), which opens new strategies for large-scale profiling of genetic interactions in mammalian cells. The CRISPRi has enormous potential for gene silencing applications. Recently, it was shown that catalytic dead Cas9 can be fused to a general repressor or activator protein such as KRAB or VP16, respectively, and thereby result in highly efficient gene silencing or activation (Gilbert et al., 2013). Furthermore, an inducible silencing system has been described, thus expanding the versatility of this approach. It is conceivable that catalytic dead Cas9 and the associated sgRNA serves as genomic targeting tools, allowing genomic site-specific modifications. The versatility of this system is very attractive, allowing modifications that reach beyond the scope of RNAi libraries. Further studies are required to address whether silencing efficiency is similar to RNAi-mediated silencing.

Overall, the three described Cas9 systems show advantages depending on the application. For instance, wild-type hCas9 seems best suited to generate gene knockouts, nickase hCas9 D10A for gene replacement strategies and catalytically dead dCas9 for gene silencing.

HIGH-THROUGHPUT SCREENING USING CRISPR/Cas9

Recent improvements have enabled the use of the CRISPR/Cas9 system as a novel tool to manipulate specific genomic regions. These developments have prompted the proposal to use this technology to set-up high-throughput screening approaches analogous to siRNA-mediated large-scale screening experiments (Qi et al., 2013). Next, we would like to consider some aspects that need to be addressed to enable the generation of large-scale CRISPR (crRNA) libraries.

(1) Design
(2) Coverage
(3) Efficiency of knockdown
(4) Off-target effects
(5) Delivery

DESIGN

Several possible configurations of the CRISPR/Cas9 system exist (see **Figure 1**). The most striking advantage for all of them is the simplicity by which a gene can be targeted. Two main components are required: first, a codon-optimized version of Cas9 endonuclease and second, the RNA components crRNA and tracrRNA. The DNA sequence encoding the crRNA has a length of about 20 nucleotides and is also known as protospacer. At the 3′ end the crRNA sequence must finish with a 2 bp (base pair) protospacer adjacent motif (PAM) of the sequence GG or AG. The crRNA sequence can be designed as complementary to the + or − strand of the target DNA region. As mentioned before it is possible to combine the crRNA sequence with the tracrRNA sequence in a sgRNA. Also CRISPR vectors for the expression of sgRNA and Cas9 from a single plasmid can be obtained from various sources via Addgene[1]. The generation of a genomic library for genome editing (using wild-type Cas9 or Cas9 nickase) or gene silencing (using catalytic inactive Cas9) can be achieved by a simple cloning of short DNA oligonucleotides into the respective CRISPR vectors. Protocols for plasmid construction and sub-cloning are freely available[2,3]. Protocols for automation of such cloning on a large-scale have previously been developed and applied to the generation of genome-wide shRNA libraries (Moffat et al., 2006). Briefly, synthesized oligonucleotide pairs coding for the desired crRNA can be annealed separately and ligated into the CRISPR vector. The ligations can be transformed into competent bacteria in a 96-well plate format. The resulting transformations from one plate can be pooled and plated onto an agar plate for robotic colony picking and plasmid sequencing. This process showed a remarkable efficiency when applied to the generation of genome-wide shRNA libraries (Moffat et al., 2006).

It should be noted that other Cas family members and Cas proteins from other organisms than *Streptococcus pyogenes* may also be suitable for gene editing purposes. This can have significant advantages in the selection of the target sequence as some Cas endonucleases have different requirements with regards to the PAM motif, which currently restricts the target efficiency of Cas9

[1] www.addgene.org
[2] http://www.addgene.org/crispr/church/
[3] http://www.genome-engineering.org/crispr/?page_id=23

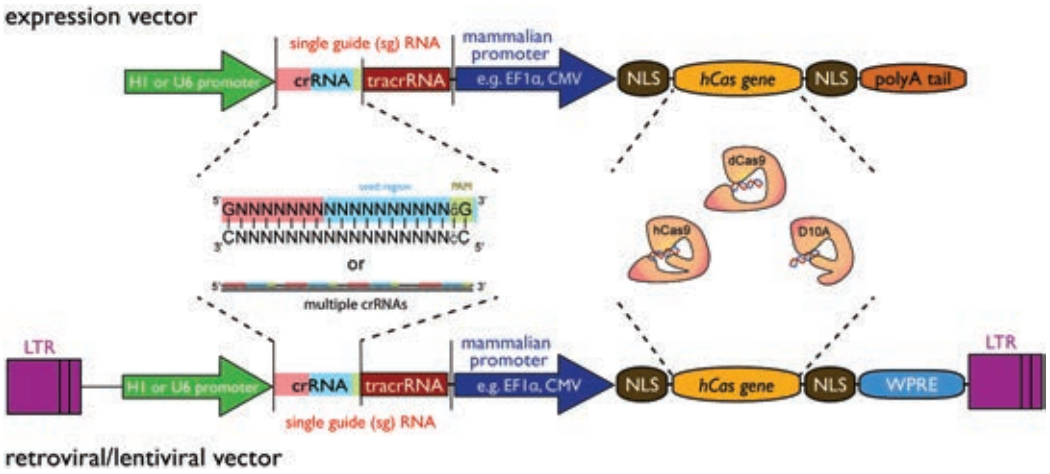

FIGURE 1 | Design principle of a CRISPR/Cas9 expression vector for construction of large-scale libraries. The vector requires two minimal components, i.e., the single-guide RNA (sgRNA) sequence and the Cas9 gene that can both be expressed from a single-vector system. The sgRNA is composed of a variable crRNA and a constant tracrRNA. The gene sequence can be inserted by a simple adaptor cloning step in the 20 bp crRNA region. Furthermore, multiple target sequences of the same gene can be inserted to increase efficiency and reduce off-target effects. At the 3′-end of the crRNA sequence, a 2 bp (base pair) protospacer adjacent motif (PAM – green box) of the sequence GG is essential, but AG may be used to a lesser extend as well. A 12 bp seed region (blue box) at the 3′-end is required for sequence targeting with additional 8 bp at the 5′-end contributing to specificity (red box). sgRNA expression can be driven by a U6 promoter or alternatively by a H1 promoter. The Cas9 component is currently available in three different forms: as a wild-type (hCas9) or a mutant (D10A) version for gene editing purposes and a catalytically dead (dCas9) version for gene silencing approaches. Expression of Cas9 can be driven by any mammalian expression promoter (e.g., EF1A, CMV, etc.) or retroviral promoter (LTR). For nuclear targeting, the Cas9 gene requires multiple nuclear localization signals (NLS) and general expression of Cas9 can be enhanced by inclusion of a woodchuck post-transcriptional regulatory element (WPRE) at the 3′-end. A polyA-tail is required for expression vectors, while it should be deleted from lenti-/retroviral expression vectors that have a polyA recognition sequence in their 3′-LTR. Variations of this design are possible with respect to the Cas gene used or further modifications such as tagging the Cas gene with GFP or NLSs in order to optimize Cas9 nuclear targeting.

to GG-PAM. For a review on sequence requirements of Cas proteins, please see Biswas et al., 2013.[4] Furthermore, improvement of Cas9 and sgRNA expression and assembly, sgRNA-5′ and 3′ modifications or nuclear targeting will readily allow for improved CRISPR efficiency.

COVERAGE

The main restriction for the design of sgRNA sequences is the PAM motif. There is strong selection for a GG motif, while the AG motif might be used to a lesser extent as well (Jiang et al., 2013). Accordingly, it was estimated that 1/8 of the genome hosts such a motif, thus enabling very high coverage of genetic regions. The Church lab has compiled a list of sites within the *Saccharomyces cerevisiae* and *H. sapiens* genome with regions suitable for incorporation into the sgRNA (Dicarlo et al., 2013; Mali et al., 2013). It was estimated that 40.5% exons of genes in the human genome have a perfect match to the *Streptococcus pyogenes* Cas9 PAM motif and ∼190,000 sgRNA-targetable sequences were identified in total (Mali et al., 2013). Using other Cas9 family members that target regions with different PAM motifs will enable a good coverage of the whole-genome. It still needs to be established how to select the best suitable sequence for each gene.

EFFICIENCY

The efficiency of gene silencing by various CRISPR/Cas9 systems has been observed to be variable and dependent on the cell type, as well as the guide RNA sequence. For instance, length and sequence complementarity of the crRNA as well as the position to which the crRNA binds within the gene locus, have been reported to affect silencing efficiency (Gilbert et al., 2013; Qi et al., 2013). Repression was inversely correlated with target distance to the transcription start site. Mali et al. observed a targeting efficiency of 10–25% in 293T cells, 13–38% in K562 cells, and 2–4% in induced pluripotent stem cells using wild-type Cas9 (Mali et al., 2013). Hwang et al. (2013) achieved a targeting efficiency of >80% in zebrafish. The CRISPRi system using catalytically inactive Cas9 achieved efficiencies of gene silencing of 46–63% in HEK293 cells and much higher in *E. coli* (Qi et al., 2013).

Overall, the efficiency of knockdown needs further improvement to about 70–80% in order to produce robust phenotypes. With improvements in transfection or lenti-/retroviral infection and expression protocols as well as sgRNA design principles, the outlook is quite promising that this will be possible. Further, the incorporation of a combination of multiple crRNA sequences into each construct might be a possibility to enhance the efficiency of knockdown.

OFF-TARGET EFFECTS

The effect of off-target silencing has been evaluated in only a few examples. The minimal length of the base-pairing region within the crRNA is 12 bp ("seed region"), which can in some cases lead to significant binding to other regions of the genome. A recent study suggests that CRISPR-based genome editing has more off-target effects than other genome editing tools such as TALENs or ZFNs

[4]http://bioanalysis.otago.ac.nz/CRISPRTarget

(Fu et al., 2013). In another study, 3-bp mismatches did not result in any detectable off-target effect for genome editing of the CCR5 locus (Cho et al., 2013). A more systematic study showed that single base and to a lesser extend two base mismatches are tolerated by SpCas9, thus potentially contributing to off-target effects (Hsu et al., 2013). The group presented algorithms to predict such off-target effects and therefore will enable the selection of target sequences with minimal off-target effects[5]. Another study that addressed the off-target effects of CRISPRi-mediated silencing using RNA-seq has shown that silencing is highly specific with minimal off-target effects (Gilbert et al., 2013). Further, combining two crRNAs drastically enhances silencing efficiency (Qi et al., 2013) and may reduce off-target effects significantly. It is conceivable that the use of different systems (wt vs. nickase vs. CRISPRi) and model organisms may result in different off-target behavior. Some studies to date suggest that CRISPR-mediated genome editing shows more off-target effects than other genome editing tools, but has similar or better target gene specificity than RNAi-based silencing. Clearly, more work needs to be done to evaluate the extent of off-target effects carefully.

DELIVERY

The combination of both Cas9 endonuclease and the sgRNA in one plasmid construct enables the use of single plasmid transfection into most standard cell lines. For primary cells, specialized protocols for delivery such as those based on electroporation or microinjection may have to be used (Marine et al., 2012; Hwang et al., 2013). Transfection-based methods can be easily automated, which enables the use of the CRISPR/Cas9 system for high-throughput screening purposes. An alternative is the use of retro- or lenti-viral transduction, although one should keep in mind that there are biosafety considerations and extra care must be taken when handling humanized Cas9 endonuclease expression constructs. The use of short-term selection such as puromycin treatment can be included to enhance selection for stronger phenotypes (Wang et al., 2013). Longer selection and differentiation protocols can even enable the generation of whole organism-based silencing effects, for instance in zebrafish or mice (Hwang et al., 2013; Wang et al., 2013).

CONCLUSION

In conclusion, the design of a whole-genome targeted sgRNA library is feasible provided that CRISPR/Cas components are further optimized to ensure high-confidence genome engineering. Clearly, more data will be generated in the coming months to evaluate carefully off-target effects and sequence requirements for efficient gene knockdown. Also, the assessment of other Cas9 proteins for genome editing and silencing will be an important step forward. It should be noted that gene knockout of essential genes may result in lethality effects, thus making the analysis of more subtle phenotypes difficult. In those cases, silencing strategies such as RNAi-mediated knockdown or CRISPRi-mediated gene repression may be beneficial. Overall, given the simplicity of use developments need to be encouraged for the design of CRISPR/Cas-based large-scale whole-genome loss-of-function screening applications. Current RNAi libraries are limited to three model organisms, i.e., human, rat, and mouse. Since CRISPR gene silencing works very well in multiple model organisms, the development of libraries for other model organisms should be particularly encouraged.

ACKNOWLEDGMENTS

This work was supported by the Medical Research Council. We thank Jennifer Doudna, Jason Mercer, and Julia Petschnigg for critically reading the manuscript.

[5]See prediction tool at www.genome-engineering.org

REFERENCES

Basset, A. R., Tibbit, C., Ponting, C. P., and Liu, J. L. (2013). Highly efficient targeted mutagenesis of *Drosophila* with the CRISPR/Cas9 system. *Cell Rep.* 4, 220–228. doi: 10.1016/j.celrep.2013.06.020

Biswas, A., Gagnon, J. N., Brouns, S. J., Fineran, P. C., and Brown, C. M. (2013). CRISPRTarget: bioinformatic prediction and analysis of crRNA targets. *RNA Biol.* 10, 817–827. doi: 10.4161/rna.24046

Buehler, E., Khan, A. A., Marine, S., Rajaram, M., Bahl, A., Burchard, J., et al. (2012). siRNA off-target effects in genome-wide screens identify signaling pathway members. *Sci. Rep.* 2, 428. doi: 10.1038/srep00428

Chang, N., Sun, C., Gao, L., Zhu, D., Xu, X., Zhu, X., et al. (2013). Genome editing with RNA-guided Cas9 nuclease in Zebrafish embryos. *Cell Res.* 23, 465–472. doi: 10.1038/cr.2013.45

Cho, S. W., Kim, S., Kim, J. M., and Kim, J.-S. (2013). Targeted genome engineering in human cells with the Cas9 RNA-guided endonuclease. *Nat. Biotechnol.* 31, 230–232. doi: 10.1038/nbt.2507

Cong, L., Ran, F. A., Cox, D., Lin, S., Barretto, R., Habib, N., et al. (2013). Multiplex genome engineering using CRISPR/Cas systems. *Science* 339, 819–823. doi: 10.1126/science.1231143

Deltcheva, E., Chylinski, K., Sharma, C. M., Gonzales, K., Chao, Y., Pirzada, Z. A., et al. (2011). CRISPR RNA maturation by trans-encoded small RNA and host factor RNase III. *Nature* 471, 602–607. doi: 10.1038/nature09886

Dicarlo, J. E., Norville, J. E., Mali, P., Rios, X., Aach, J., and Church, G. M. (2013). Genome engineering in *Saccharomyces cerevisiae* using CRISPR-Cas systems. *Nucleic Acids Res.* 41, 4336–4343. doi: 10.1093/nar/gkt135

Friedland, A. E., Tzur, Y. B., Esvelt, K. M., Colaiacovo, M. P., Church, G. M., and Calarco, J. A. (2013). Heritable genome editing in *C. elegans* via a CRISPR-Cas9 system. *Nat. Methods* 10, 741–743. doi: 10.1038/nmeth.2532

Fu, Y., Foden, J. A., Khayter, C., Maeder, M. L., Reyon, D., Joung, J. K., et al. (2013). High-frequency off-target mutagenesis induced by CRISPR-Cas nucleases in human cells. *Nat. Biotechnol.* 31, 822–826. doi: 10.1038/nbt.2623

Gilbert, L. A., Larson, M. H., Morsut, L., Liu, Z., Brar, G. A., Torres, S. E., et al. (2013). CRISPR-mediated modular RNA-guided regulation of transcription in eukaryotes. *Cell* 154, 442–451. doi: 10.1016/j.cell.2013.06.044

Gil-Humanes, J., Piston, F., Tollefsen, S., Sollid, L. M., and Barro, F. (2010). Effective shutdown in the expression of celiac disease-related wheat gliadin T-cell epitopes by RNA interference. *Proc. Natl. Acad. Sci. U.S.A.* 107, 17023–17028. doi: 10.1073/pnas.1007773107

Gratz, S., Cummings, A., Nguyen, J., Hamm, D., Donohue, L., Harrison, M., et al. (2013). Genome engineering of *Drosophila* with the CRISPR RNA-guided Cas9 nuclease. *Genetics* 194, 1029–1035. doi: 10.1534/genetics.113.152710

Hsu, P. D., Scott, D. A., Weinstein, J. A., Ran, F. A., Konermann, S., Agarwala, V., et al. (2013). DNA targeting specificity of RNA-guided Cas9 nucleases. *Nat. Biotechnol.* 31, 827–832. doi: 10.1038/nbt.2647

Hwang, W. Y., Fu, Y., Reyon, D., Maeder, M. L., Tsai, S. Q., Sander, J. D., et al. (2013). Efficient genome editing in zebrafish using a CRISPR-Cas system. *Nat. Biotechnol.* 31, 227–229. doi: 10.1038/nbt.2501

Jiang, W., Bikard, D., Cox, D., Zhang, F., and Marraffini, L. A. (2013). RNA-guided editing of

bacterial genomes using CRISPR-Cas systems. *Nat. Biotechnol.* 31, 233–239. doi: 10.1038/nbt.2508

Jinek, M., Chylinski, K., Fonfara, I., Hauer, M., Doudna, J. A., and Charpentier, E. (2012). A programmable dual-RNA-guided DNA endonuclease in adaptive bacterial immunity. *Science* 337, 816–821. doi: 10.1126/science.1225829

Jinek, M., East, A., Cheng, A., Lin, S., Ma, E., and Doudna, J. (2013). RNA-programmed genome editing in human cells. *eLife* 2, e00471. doi: 10.7554/eLife.00471

Ketteler, R. (2012). On programmed ribosomal frameshifting: the alternative proteomes. *Front. Genet.* 3:242. doi: 10.3389/fgene.2012.00242

Li, D., Qiu, Z., Shao, Y., Chen, Y., Guan, Y., Liu, M., et al. (2013a). Heritable gene targeting in the mouse and rat using a CRISPR-Cas system. *Nat. Biotechnol.* 31, 681–683. doi: 10.1038/nbt.2661

Li, J. F., Norville, J. E., Aach, J., McCormack, M., Zhang, D., Bush, J., et al. (2013b). Multiplex and homologous recombination-mediated genome editing in Arabidopsis and *Nicotiana benthamiana* using guide RNA and Cas9. *Nat. Biotechnol.* 31, 688–691. doi: 10.1038/nbt.2654

Li, W., Teng, F., Li, T., and Zhou, Q. (2013c). Simultaneous generation and germline transmission of multiple gene mutations in rat using CRISPR-Gas systems. *Nat. Biotechnol.* 31, 684–686. doi: 10.1038/nbt.2652

Mali, P., Yang, L., Esvelt, K. M., Aach, J., Guell, M., DiCarlo, J. E., et al. (2013). RNA-guided human genome engineering via Cas9. *Science* 339, 823–826. doi: 10.1126/science.1232033

Marine, S., Bahl, A., Ferrer, M., and Buehler, E. (2012). Common seed analysis to identify off-target effects in siRNA screens. *J. Biomol. Screen.* 17, 370–378. doi: 10.1177/1087057111427348

Moffat, J., Grueneberg, D. A., Yang, X., Kim, S. Y., Kloepfer, A. M., Hinkle, G., et al. (2006). A lentiviral RNAi library for human and mouse genes applied to an arrayed viral high-content screen. *Cell* 124, 1283–1298. doi: 10.1016/j.cell.2006.01.040

Nekrasov, V., Staskawicz, B., Weigel, D., Jones, J. D. G., and Kamoun, S. (2013). Targeted mutagenesis in the model plant *Nicotiana benthamiana* using Cas9 RNA-guided endonuclease. *Nat. Biotechnol.* 31, 691–693. doi: 10.1038/nbt.2655

Qi, L. S., Larson, M. H., Gilbert, L. A., Doudna, J. A., Weissman, J. S., Arkin, A. P., et al. (2013). Repurposing CRISPR as an RNA-guided platform for sequence-specific control of gene expression. *Cell* 152, 1173–1183. doi: 10.1016/j.cell.2013.02.022

Ramalingam, S., Annaluru, N., and Chandrasegaran, S. (2013). A CRISPR way to engineer the human genome. *Genome Biol.* 14. 107. doi: 10.1186/gb-2013-14-2-107

Reyon, D., Tsai, S. Q., Khayter, C., Foden, J. A., Sander, J. D., and Joung, J. K. (2012). FLASH assembly of TALENs for high-throughput genome editing. *Nat. Biotechnol.* 30, 460–465. doi: 10.1038/nbt.2170

Seed, B. (1995). Developments in expression cloning. *Curr. Opin. Biotechnol.* 6, 567–573. doi: 10.1016/0958-1669(95)80094-8

Shan, Q., Wang, Y., Li, J., Zhang, Y., Chen, K., Liang, Z., et al. (2013). Targeted genome modification of crop plants using a CRISPR-Cas system. *Nat. Biotechnol.* 31, 686–688. doi: 10.1038/nbt.2650

Sorek, R., Lawrence, C., and Wiedenheft, B. (2013). CRISPR-mediated adaptive immune systems in bacteria and archaea. *Annu. Rev. Biochem.* 82, 237–266. doi: 10.1146/annurev-biochem-072911-172315

Wang, H., Yang, H., Shivalila, C. S., Dawlaty, M. M., Cheng, A. W., Zhang, F., et al. (2013). One-step generation of mice carrying mutations in multiple genes by CRISPR/Cas-mediated genome engineering. *Cell* 153, 910–918. doi: 10.1016/j.cell.2013.04.025

Yu, Z., Ren, M., Wang, Z., Zhang, B., Rong, Y. S., Jiao, R., et al. (2013). Highly efficient genome modifications mediated by CRISPR/Cas9 in *Drosophila*. *Genetics* 195, 289–291. doi:10.1534/genetics.113.153825 doi: 10.1534/genetics.113.153825

Conflict of Interest Statement: The authors declare that the research was conducted in the absence of any commercial or financial relationships that could be construed as a potential conflict of interest.

Received: 13 June 2013; accepted: 12 September 2013; published online: 07 October 2013.

Citation: Heintze J, Luft C and Ketteler R (2013) A CRISPR CASe for high-throughput silencing. Front. Genet. ***4****:193. doi: 10.3389/fgene.2013.00193*

This article was submitted to Genomic Assay Technology, a section of the journal Frontiers in Genetics.

SCIENCE ADVANCES | RESEARCH ARTICLE

GENETICS

CRISPR-Cpf1 correction of muscular dystrophy mutations in human cardiomyocytes and mice

Yu Zhang,[1,2,3]* Chengzu Long,[1,2,3]*†‡ Hui Li,[1,2,3] John R. McAnally,[1,2,3] Kedryn K. Baskin,[1,2,3] John M. Shelton,[4] Rhonda Bassel-Duby,[1,2,3] Eric N. Olson[1,2,3]‡

Duchenne muscular dystrophy (DMD), caused by mutations in the X-linked dystrophin gene (*DMD*), is characterized by fatal degeneration of striated muscles. Dilated cardiomyopathy is one of the most common lethal features of the disease. We deployed Cpf1, a unique class 2 CRISPR (clustered regularly interspaced short palindromic repeats) effector, to correct *DMD* mutations in patient-derived induced pluripotent stem cells (iPSCs) and *mdx* mice, an animal model of DMD. Cpf1-mediated genomic editing of human iPSCs, either by skipping of an out-of-frame *DMD* exon or by correcting a nonsense mutation, restored dystrophin expression after differentiation to cardiomyocytes and enhanced contractile function. Similarly, pathophysiological hallmarks of muscular dystrophy were corrected in *mdx* mice following Cpf1-mediated germline editing. These findings are the first to show the efficiency of Cpf1-mediated correction of genetic mutations in human cells and an animal disease model and represent a significant step toward therapeutic translation of gene editing for correction of DMD.

INTRODUCTION

Duchenne muscular dystrophy (DMD) is an X-linked recessive disease caused by mutations in the gene coding for dystrophin, which is a large cytoskeletal protein essential for the integrity of muscle cell membranes (*1*). DMD causes progressive muscle weakness, culminating in premature death by the age of 30 years, generally from cardiomyopathy. There is no effective treatment for this disease. Numerous approaches to rescue dystrophin expression in DMD have been attempted, including delivery of truncated dystrophin or utrophin by recombinant adeno-associated virus (AAV) (*2*, *3*) and skipping of mutant exons with antisense oligonucleotides and small molecules (*4*). However, these approaches cannot correct *DMD* mutations or permanently restore dystrophin expression.

The CRISPR (clustered regularly interspaced short palindromic repeats) system functions as an adaptive immune system in bacteria and archaea that defends against phage infection (*5*). In this system, an endonuclease is guided to specific genomic sequences by a single guide RNA (sgRNA), resulting in DNA cutting near a protospacer adjacent motif (PAM) sequence. The CRISPR-Cas (CRISPR-associated proteins) system represents a promising approach for correction of diverse genetic defects (*6*–*12*). However, many challenges remain to be addressed. For example, *Streptococcus pyogenes* Cas9 (SpCas9), currently the most widely used Cas9 endonuclease, has a G-rich PAM requirement (NGG) that excludes genome editing of AT-rich regions (*13*). Additionally, the large size of SpCas9 reduces the efficiency of packaging and delivery in low-capacity viral vectors, such as AAV vectors. The Cas9 endonuclease from *Staphylococcus aureus* (SaCas9), although smaller in size than SpCas9, has a PAM sequence (NNGRRT) that is longer and more complex, thus limiting the range of its genomic targets (*13*). Smaller CRISPR enzymes with greater flexibility in recognition sequence and comparable cutting efficiency would facilitate precision gene editing, especially for translational applications.

Recently, a new RNA-guided endonuclease, named Cpf1 (CRISPR from *Prevotella* and *Francisella* 1), was shown to be effective in mammalian genome cleavage (*14*–*18*). Cpf1 has several unique features that expand its genome editing potential: (i) Cpf1-mediated cleavage is guided by a single and short crRNA (abbreviated as gRNA), whereas Cas9-mediated cleavage is guided by a hybrid of CRISPR RNA (crRNA) and a long trans-activating crRNA (tracrRNA) (*19*). (ii) Cpf1 prefers a T-rich PAM at the 5′ end of a protospacer, whereas Cas9 requires a G-rich PAM at the 3′ end of the target sequence. (iii) Cpf1-mediated cleavage produces a sticky end distal to the PAM site, which activates DNA repair machinery, whereas Cas9 cutting generates a blunt end. (iv) Cpf1 also has ribonuclease activity, which can process precursor crRNAs to mature crRNAs (*14*, *20*). Like Cas9, Cpf1 binds to a targeted genomic site and generates a double-stranded break, which is then repaired either by nonhomologous end joining (NHEJ) or by homology-directed repair (HDR) if an exogenous template is provided. Although Cpf1 has been shown to be active in mammalian genome editing (*14*–*17*), its potential usefulness for correction of genetic mutations in mammalian cells and animal models of disease has yet to be demonstrated.

Previously, we and others used CRISPR-Cas9 to correct the *DMD* mutation in mice and human cells (*7*, *9*, *10*, *21*–*23*). Here, we show that Cpf1 provides a robust and efficient RNA-guided genome editing system that can be used to permanently correct *DMD* mutations by different strategies, thereby restoring dystrophin expression and preventing progression of the disease. These findings provide a new approach for the permanent correction of human genetic mutations.

RESULTS

Correction of DMD iPSC-derived cardiomyocytes by Cpf1-mediated genome editing

Exon deletions preceding exon 51 of the human *DMD* gene, which disrupt the open reading frame (ORF) by juxtaposing out-of-frame exons, represent the most common type of human DMD mutation (*24*). Skipping of exon 51 can, in principle, restore the DMD ORF in 13% of DMD patients with exon deletions (*25*). To test the potential of Cpf1

[1]Department of Molecular Biology, University of Texas Southwestern Medical Center, Dallas, TX 75390, USA. [2]Senator Paul D. Wellstone Muscular Dystrophy Cooperative Research Center, University of Texas Southwestern Medical Center, Dallas, TX 75390, USA. [3]Hamon Center for Regenerative Science and Medicine, University of Texas Southwestern Medical Center, Dallas, TX 75390, USA. [4]Department of Internal Medicine, University of Texas Southwestern Medical Center, Dallas, TX 75390, USA.
*These authors contributed equally to this work.
†Present address: Leon H. Charney Division of Cardiology, New York University School of Medicine, New York, NY 10016, USA.
‡Corresponding author. Email: Eric.Olson@UTSouthwestern.edu (E.N.O.); Chengzu.Long@nyumc.org (C.L.)

to correct this type of "hotspot" mutation, we used DMD patient fibroblast-derived induced pluripotent stem cells (iPSCs) (Riken HPS0164; abbreviated as Riken51), which harbor a deletion of exons 48 to 50, introducing a premature termination codon within exon 51 (Fig. 1A).

The splice acceptor region is generally pyrimidine-rich (*26*), which creates an ideal PAM sequence for genome editing by Cpf1 endonuclease (Fig. 1B). To rescue dystrophin expression in Riken51 iPSCs, we used a Cpf1 gRNA to target exon 51, introducing small insertions and deletions (INDELs) in exon 51 by NHEJ and subsequently reframing the dystrophin ORF, theoretically, in one-third of corrected genes, a process we refer to as "reframing" (Fig. 1A). We also compared two Cpf1 orthologs, LbCpf1 (from *Lachnospiraceae bacterium ND2006*) and AsCpf1 (from *Acidaminococcus sp. BV3L6*), which use the same PAM sequences for genome cleavage.

Cpf1 cleavage was targeted near the T-rich splice acceptor site of exon 51 using a gRNA (designated g1) (Fig. 1C), which was cloned into the pLbCpf1-2A-GFP and pAsCpf1-2A-GFP plasmids (Fig. 1D). These plasmids express human codon-optimized LbCpf1 or AsCpf1, plus green fluorescent protein (GFP), enabling fluorescence-activated cell sorting (FACS) of Cpf1-expressing cells (Fig. 1D). Initially, we evaluated the cleavage efficiency of Cpf1 editing with g1 in human 293T cells. Both LbCpf1 and AsCpf1 efficiently induced DNA cleavage with g1, as detected using the T7E1 assay that recognizes and cleaves non-perfectly matched DNA (Fig. 1E).

Next, we used LbCpf1 and AsCpf1 with g1 to edit Riken51 iPSCs, and using the T7E1 assay, we observed genome cleavage at *DMD* exon 51 (Fig. 1E). Genomic polymerase chain reaction (PCR) products from the Cpf1-edited *DMD* exon 51 were cloned and sequenced (fig. S1A). We observed INDELs near the exon 51 splice acceptor site in both LbCpf1- and AsCpf1-edited Riken51 iPSCs (fig. S1A). Single clones from a mixture of reframed Riken51 iPSCs were picked and expanded, and the edited genomic region was sequenced. Of the 12 clones, we observed 4 clones with reframed *DMD* exon 51, which restored the ORF (fig. S1B).

Restoration of dystrophin expression in DMD iPSC-derived cardiomyocytes after Cpf1-mediated reframing

Riken51 iPSCs edited by CRISPR-Cpf1 using the reframing strategy were induced to differentiate into cardiomyocytes (Fig. 2A) (*27*). Cardiomyocytes with the reframed *DMD* gene were identified by reverse transcription PCR (RT-PCR) using a forward primer targeting exon 47 and a reverse primer targeting exon 52, and the PCR products were sequenced (Fig. 2, B and C). Uncorrected iPSC-derived cardiomyocytes have a premature termination codon following the first eight amino acids encoded by exon 51 (Fig. 2C). Cardiomyocytes differentiated from Cpf1-edited Riken51 iPSCs showed restoration of the *DMD* ORF, as seen by sequencing of the RT-PCR products from amplification of exons 47 to 52 (Fig. 2C). We also confirmed restoration of dystrophin protein expression by Western blot analysis and immunocytochemistry using a dystrophin antibody (Fig. 2, D and E). Even without clonal selection and expansion, cardiomyocytes differentiated from Cpf1-edited iPSC mixtures showed levels of dystrophin protein comparable to wild-type (WT) cardiomyocytes (Fig. 2D).

From mixtures of LbCpf1-edited Riken51 iPSCs, we picked two clones (clones #2 and #5) with in-frame INDELs of different sizes and differentiated the clones into cardiomyocytes. Clone #2 had an 8-bp deletion at the 5′ end of exon 51, together with an endogenous deletion of exons 48 to 50. The total 405-bp deletion restored the *DMD*

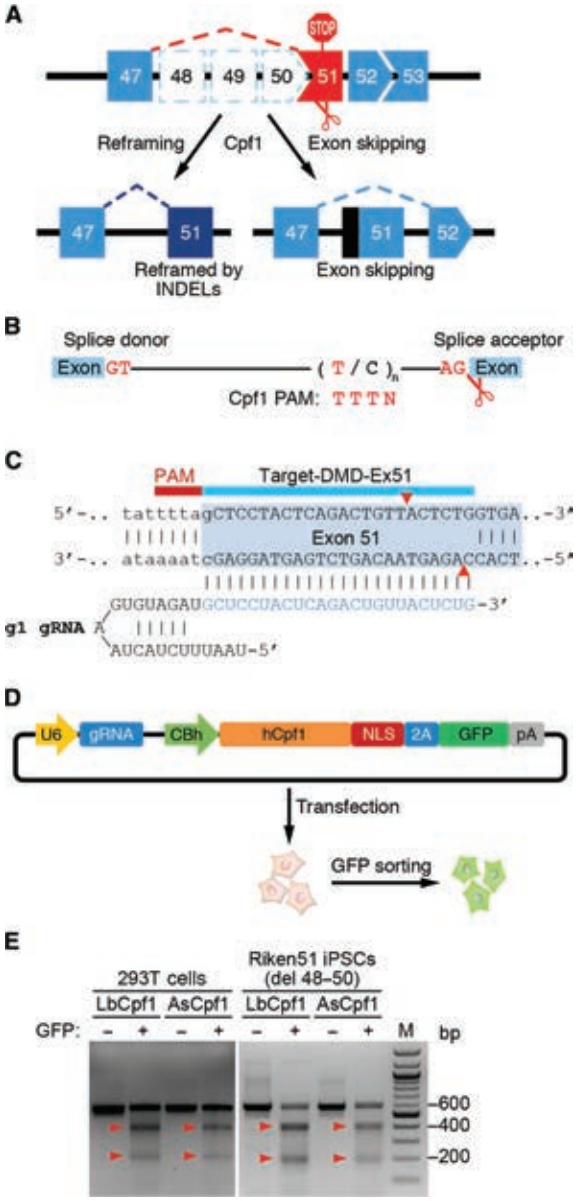

Fig. 1. Correction of DMD mutations by Cpf1-mediated genome editing. (**A**) A *DMD* deletion of exons 48 to 50 results in splicing of exons 47 to 51, generating an out-of-frame mutation of dystrophin. Two strategies were used for the restoration of dystrophin expression by Cpf1. In the "reframing" strategy, small INDELs in exon 51 restore the protein reading frame of dystrophin. The "exon skipping" strategy is achieved by disruption of the splice acceptor of exon 51, which results in splicing of exons 47 to 52 and restoration of the protein reading frame. (**B**) The 3′ end of an intron is T-rich, which generates Cpf1 PAM sequences, enabling genome cleavage by Cpf1. (**C**) Illustration of Cpf1 gRNA targeting *DMD* exon 51. The T-rich PAM (red line) is located upstream of exon 51 near the splice acceptor site. The sequence of the Cpf1 g1 gRNA targeting exon 51 is shown, highlighting the complementary nucleotides in blue. Cpf1 cleavage produces a staggered end distal to the PAM site (demarcated by red arrowheads). The 5′ region of exon 51 is shaded in light blue. Exon sequence is in uppercase letters. Intron sequence is in lowercase letters. (**D**) Illustration of a plasmid encoding human codon-optimized Cpf1 (hCpf1) with a nuclear localization signal (NLS) and 2A-GFP, driven by a hybrid form of cytomegalovirus and chicken β-actin promoters (CBh). The plasmid also encodes a Cpf1 gRNA driven by the U6 promoter. Cells transfected with this plasmid express GFP, allowing for selection of Cpf1-expressing cells by FACS. (**E**) T7E1 assays using human 293T cells or DMD iPSCs (Riken51) transfected with plasmid expressing LbCpf1 or AsCpf1, gRNA, and GFP show genome cleavage at *DMD* exon 51. Red arrowheads point to cleavage products. M, marker; bp, base pair.

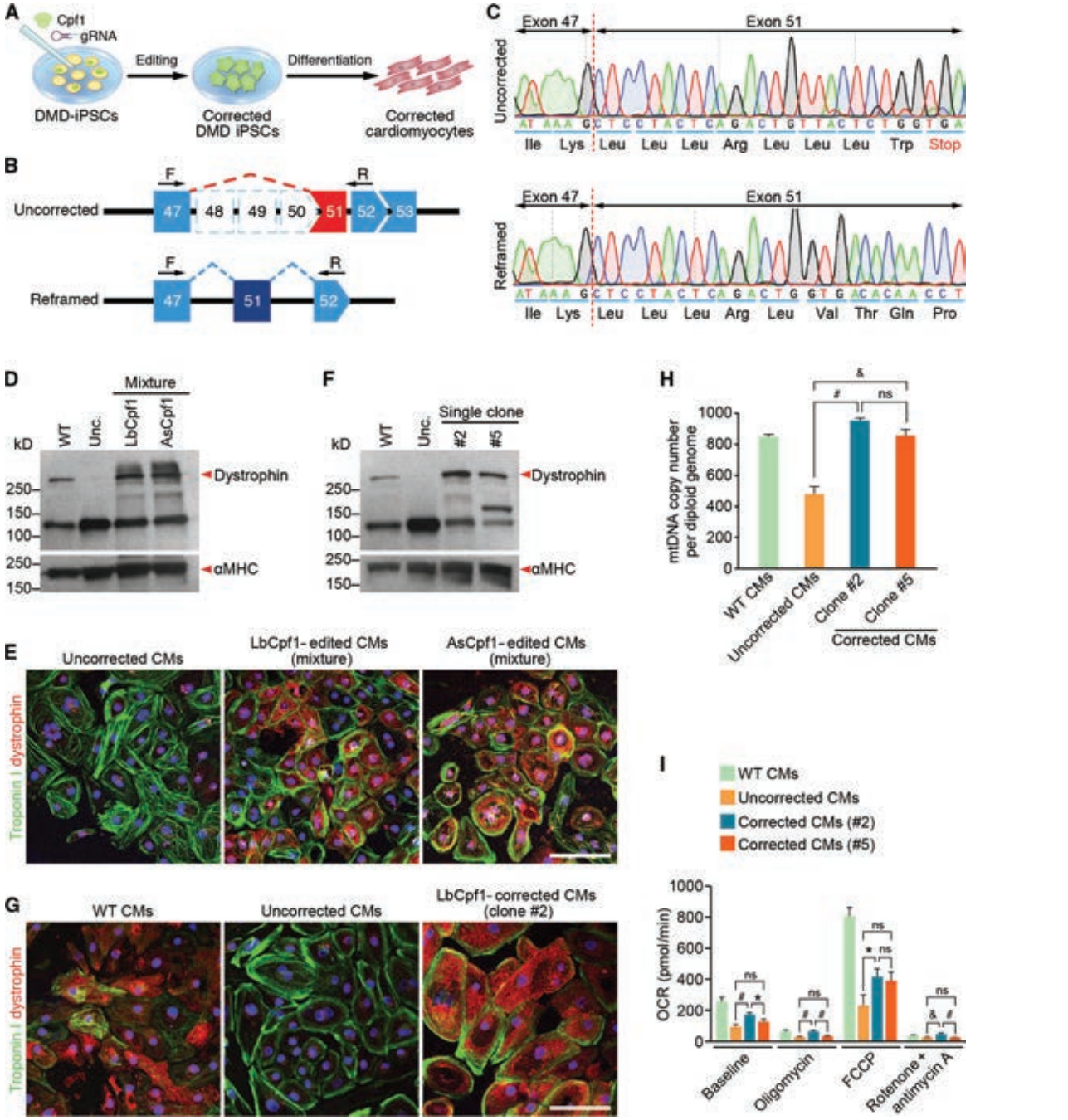

Fig. 2. DMD iPSC-derived cardiomyocytes express dystrophin after Cpf1-mediated genome editing by reframing. (**A**) DMD skin fibroblast-derived iPSCs were edited by Cpf1 using gRNA (corrected DMD iPSCs) and then differentiated into cardiomyocytes (corrected cardiomyocytes) for analysis of genetic correction of the *DMD* mutation. (**B**) A *DMD* deletion of exons 48 to 50 results in splicing of exon 47 to 51, generating an out-of-frame mutation of dystrophin. Forward primer (F) targeting exon 47 and reverse primer (R) targeting exon 52 were used in RT-PCR to confirm the reframing strategy by Cpf1-meditated genome editing in cardiomyocytes. Uncorrected cardiomyocytes lack exons 48 to 50. In contrast, after reframing, exon 51 is placed back in frame with exon 47. (**C**) Sequencing of representative RT-PCR products shows that uncorrected DMD iPSC-derived cardiomyocytes have a premature stop codon in exon 51, which creates a nonsense mutation. After Cpf1-mediated reframing, the ORF of dystrophin is restored. Dashed red line denotes exon boundary. (**D**) Western blot analysis shows dystrophin expression in a mixture of DMD iPSC-derived cardiomyocytes edited by reframing with LbCpf1 or AsCpf1 and g1 gRNA. Even without clonal selection, Cpf1-mediated reframing is efficient and sufficient to restore dystrophin expression in the cardiomyocyte mixture. α-Myosin heavy chain (αMHC) is loading control. (**E**) Immunocytochemistry shows dystrophin expression in iPSC-derived cardiomyocyte (CM) mixtures following LbCpf1- or AsCpf1-mediated reframing. Red, dystrophin staining; green, troponin I staining. Scale bar, 100 μm. (**F**) Western blot analysis shows dystrophin expression in single clones (#2 and #5) of iPSC-derived cardiomyocytes following clonal selection after LbCpf1-mediated reframing. αMHC is loading control. (**G**) Immunocytochemistry shows dystrophin expression in clone #2 LbCpf1-edited iPSC-derived cardiomyocytes. Scale bar, 100 μm. (**H**) Quantification of mtDNA copy number in single clones (#2 and #5) of LbCpf1-edited iPSC-derived cardiomyocytes. Data are means ± SEM ($n = 3$). $^{\&}P < 0.01$ and $^{\#}P < 0.005$. ns, not significant. (**I**) Basal OCR of single clones (#2 and #5) of LbCpf1-edited iPSC-derived cardiomyocytes, and OCR in response to oligomycin, FCCP, rotenone, and antimycin A, normalized to cell number. Data are means ± SEM ($n = 5$). $^{*}P < 0.05$, $^{\&}P < 0.01$, and $^{\#}P < 0.005$.

ORF and allowed for the production of a truncated dystrophin protein with a 135–amino acid deletion. Clone #5 had a 17-bp deletion in exon 51 and produced dystrophin protein with a 138–amino acid deletion. Although there is high efficiency of cleavage by Cpf1, the amount of DNA inserted or deleted at the cleavage site varies. Additionally, INDELs can generate extra codons at the edited locus, causing changes of the ORF. The dystrophin protein expressed by clone #2 cardiomyocytes generated an additional four amino acids (Leu-Leu-Leu-Arg) between exon 47 and exon 51, whereas dystrophin protein expressed by clone #5 cardiomyocytes generated only one additional amino acid (Leu). From both clones #2 and #5, we observed restored dystrophin protein by Western blot analysis and immunocytochemistry (Fig. 2, F and G). Because of the large size of dystrophin, the internally deleted forms migrated similarly to WT dystrophin on SDS–polyacrylamide gel electrophoresis.

We also performed functional analysis of DMD iPSC-derived cardiomyocytes by measuring mitochondrial DNA (mtDNA) copy number and cellular respiration rates. Uncorrected DMD iPSC-derived cardiomyocytes had significantly fewer mitochondria than the LbCpf1-corrected cardiomyocytes (Fig. 2H). After LbCpf1-mediated reframing, both corrected clones restored mitochondrial number to a level comparable to that of WT cardiomyocytes (Fig. 2H). Clone #2 iPSC-derived cardiomyocytes also showed an increase in oxygen consumption rate (OCR) compared to uncorrected iPSC-derived cardiomyocytes at baseline (Fig. 2I). OCR was inhibited by oligomycin in all iPSC-derived cardiomyocytes, and treatment with the uncoupling agent FCCP (carbonyl cyanide *p*-trifluoromethoxyphenylhydrazone) enhanced OCR. Finally, treatment with rotenone and antimycin A further inhibited OCR in all cardiomyocytes. These results demonstrate that Cpf1-mediated *DMD* correction improved respiratory capacity of mitochondria in corrected iPSC-derived cardiomyocytes. Our findings show that Cpf1-mediated reframing is a highly efficient strategy to rescue DMD phenotypes in human cardiomyocytes.

Restoration of dystrophin expression in DMD iPSC-derived cardiomyocytes by Cpf1-mediated exon skipping

In contrast to the single gRNA-mediated reframing method, which introduces small INDELs, exon skipping uses two gRNAs to disrupt splice sites and generates a large deletion (Fig. 3A). As an independent strategy to restore dystrophin expression in the Riken51 iPSCs, we designed two LbCpf1 gRNAs (g2 and g3) that target the 3′ end of intron 50 and tested the cleavage efficiency in human 293T cells. The T7E1 assay showed that g2 had higher cleavage efficiency within intron 50 compared to g3 (Fig. 3B). Therefore, we co-delivered LbCpf1, g2, and g1 (g1 targets the 5′ region of exon 51) into Riken51 iPSCs, with the aim of disrupting the splice acceptor site of exon 51. Genomic PCR showed a lower band in LbCpf1-edited iPSCs (Fig. 3C), and sequencing data confirmed the presence of a deletion of ~200 bp between intron 50 and exon 51, which disrupted the conserved splice acceptor site (Fig. 3D).

Targeting specificity of Cpf1 was evaluated using the top 10 potential genome-wide off-target sites (OT-01 to OT-10) for each gRNA, as predicted by Cas-OFFinder (www.rgenome.net/cas-offinder/) (tables S1 and S2). Efficient cleavage bands were observed at the on-target site, and most of the off-target sites did not show a detectable cleavage band by the T7E1 assay (fig. S2) or by quantitative capillary electrophoresis using a fragment analyzer (figs. S3 and S4).

Riken51 iPSCs edited by the exon skipping strategy with g1 and g2 were differentiated into cardiomyocytes. Cells harboring the edited *DMD* allele were identified by RT-PCR using a forward primer targeting exon 47 and a reverse primer targeting exon 52, showing deletion of the exon

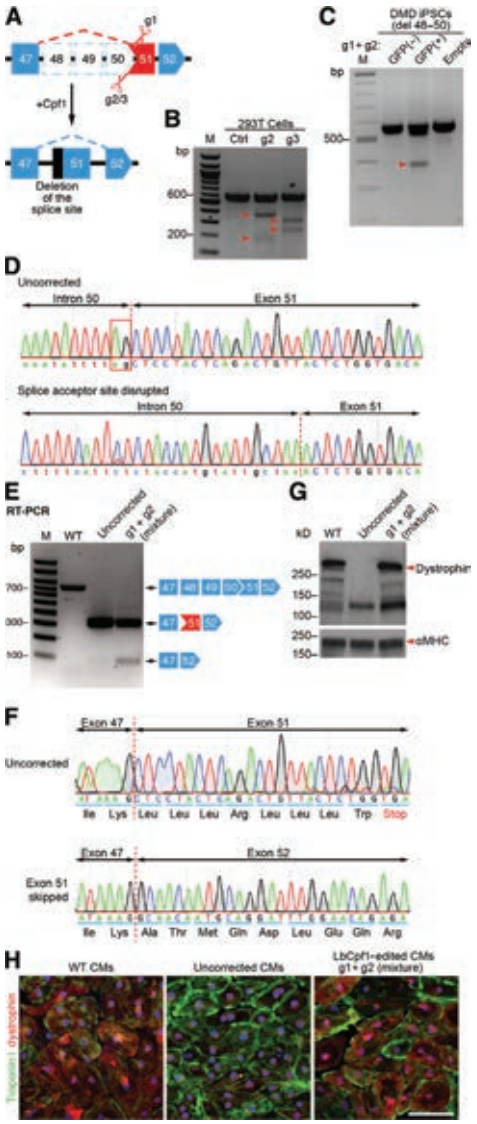

Fig. 3. DMD iPSC-derived cardiomyocytes express dystrophin after Cpf1-mediated exon skipping. (**A**) Two gRNAs [either gRNA (g2 or g3), which target intron 50, and the other (g1), which targets exon 51] were used to direct Cpf1-mediated removal of the exon 51 splice acceptor site. (**B**) T7E1 assay using 293T cells transfected with LbCpf1 and gRNA2 (g2) or gRNA3 (g3) shows cleavage of the *DMD* locus at intron 50. Red arrowheads denote cleavage products. M, marker; Ctrl, control. (**C**) PCR products of genomic DNA isolated from DMD-iPSCs transfected with a plasmid expressing LbCpf1, g1 + g2, and GFP. The lower band (red arrowhead) indicates removal of the exon 51 splice acceptor site. (**D**) Sequence of the lower PCR band from (C) shows a 200-bp deletion, spanning from the 3′ end of intron 50 to the 5′ end of exon 51. This confirms removal of the "ag" splice acceptor of exon 51. The sequence of the uncorrected allele is shown above that of the LbCpf1-edited allele. (**E**) RT-PCR of iPSC-derived cardiomyocytes using primer sets described in Fig. 2B. The 700-bp band in the WT lane is the dystrophin transcript from exons 47 to 52; the 300-bp band in the uncorrected lane is the dystrophin transcript from exons 47 to 52 with exon 48 to 50 deletion; and the lower band in the g1 + g2 mixture lane (edited by LbCpf1) shows exon 51 skipping. (**F**) Sequence of the lower band from (E) (g1 + g2 mixture lane) confirms skipping of exon 51, which reframed the *DMD* ORF. (**G**) Western blot analysis shows dystrophin protein expression in iPSC-derived cardiomyocyte mixtures after exon 51 skipping by LbCpf1 with g1 + g2. αMHC is loading control. (**H**) Immunocytochemistry shows dystrophin expression in iPSC-derived cardiomyocyte mixtures following Cpf1-mediated exon skipping with g1 + g2 gRNA compared to WT and uncorrected cardiomyocyte mixtures. Red, dystrophin staining; green, troponin I staining. Scale bar, 100 μm.

51 splice acceptor site, which allows skipping of exon 51 (Fig. 3E). Sequencing of the RT-PCR products confirmed that exon 47 was spliced to exon 52, which restored the *DMD* ORF (Fig. 3F). Western blot analysis and immunocytochemistry confirmed the restoration of dystrophin protein expression in a mixture of LbCpf1-edited cardiomyocytes with g1 and g2 (Fig. 3, G and H). Thus, Cpf1 editing by the exon skipping strategy is highly efficient in rescuing the DMD phenotype in human cardiomyocytes.

Restoration of dystrophin in *mdx* mice by Cpf1-mediated correction

To further evaluate the potential of Cpf1-mediated *Dmd* correction in vivo, we used LbCpf1 to permanently correct the mutation in the germ line of *mdx* mice by HDR-mediated correction or NHEJ-mediated reframing. *mdx* mice carry a nonsense mutation in exon 23 of the *Dmd* gene because of a C-to-T transition (Fig. 4A). Three gRNAs (g1, g2, and g3) that target exon 23 were screened and tested in mouse 10T1/2 fibroblasts for cleavage efficiency (Fig. 4B). The T7E1 assay revealed that LbCpf1 and AsCpf1 had different cleavage efficiencies at *Dmd* exon 23 (Fig. 4C). On the basis of sequencing results, LbCpf1-mediated genome editing using g2 generated a greater occurrence of INDELs in mouse fibroblasts compared to g3 (fig. S1C).

LbCpf1 editing with g2 recognizes a PAM sequence 9 bp upstream of the mutation site and creates a staggered double-stranded DNA cut 8 bp downstream of the mutation site (Fig. 4D). To obtain HDR genome editing, we used a 180-bp single-stranded oligodeoxynucleotide (ssODN) in combination with LbCpf1 and g2, because it has been shown that ssODNs are more efficient in introducing small genomic modifications than double-stranded donor plasmids (*6*, *7*). We generated an ssODN containing 90 bp of sequence homology flanking the cleavage site, including four silent mutations and a Tse I restriction site to facilitate genotyping, as previously described (*7*). This ssODN was designed to be used with LbCpf1 and g2 to correct the C-to-T mutation within *Dmd* exon 23 and to restore dystrophin in *mdx* mice by HDR.

Correction of muscular dystrophy in *mdx* mice by LbCpf1-mediated HDR or NHEJ

mdx zygotes were coinjected with in vitro transcribed LbCpf1 mRNA, in vitro transcribed g2 gRNA, and 180-bp ssODN and reimplanted into pseudopregnant females (Fig. 5A). Three litters of LbCpf1-edited *mdx* mice were analyzed by the T7E1 assay and Tse I RFLP (restriction fragment length polymorphism) (Fig. 5, B and C). Of the 24 pups born, 12 were T7E1-positive and 5 carried corrected alleles (*mdx*-C1 to *mdx*-C5), as detected by Tse I RFLP and sequencing (Fig. 5, C and D). Skeletal muscles (tibialis anterior and gastrocnemius/plantaris) from WT, *mdx*, and LbCpf1-corrected *mdx*-C mice were analyzed at 4 weeks of age. Hematoxylin and eosin (H&E) staining of muscle showed fibrosis and inflammatory infiltration in *mdx* muscle, whereas LbCpf1-corrected (*mdx*-C) muscle displayed normal muscle morphology and no signs of a dystrophic phenotype (Fig. 5E and fig. S5, A and B). Immunohistochemistry showed the absence of dystrophin-positive fibers in muscle sections of *mdx* mice, whereas *mdx*-C muscle corrected by LbCpf1-mediated HDR showed dystrophin protein expression in a majority of muscle fibers (Fig. 5F and fig. S5, A and B).

Additionally, we performed histological analysis of different tissues from multiple *mdx*-C mice with correction rates from 8 to 50%. All LbCpf1-corrected *mdx*-C mice showed restored dystrophin expression in multiple tissues, including skeletal muscles, heart, and brain (figs. S6 and S7). Muscle of *mdx*-C mice with 50% genomic correction showed

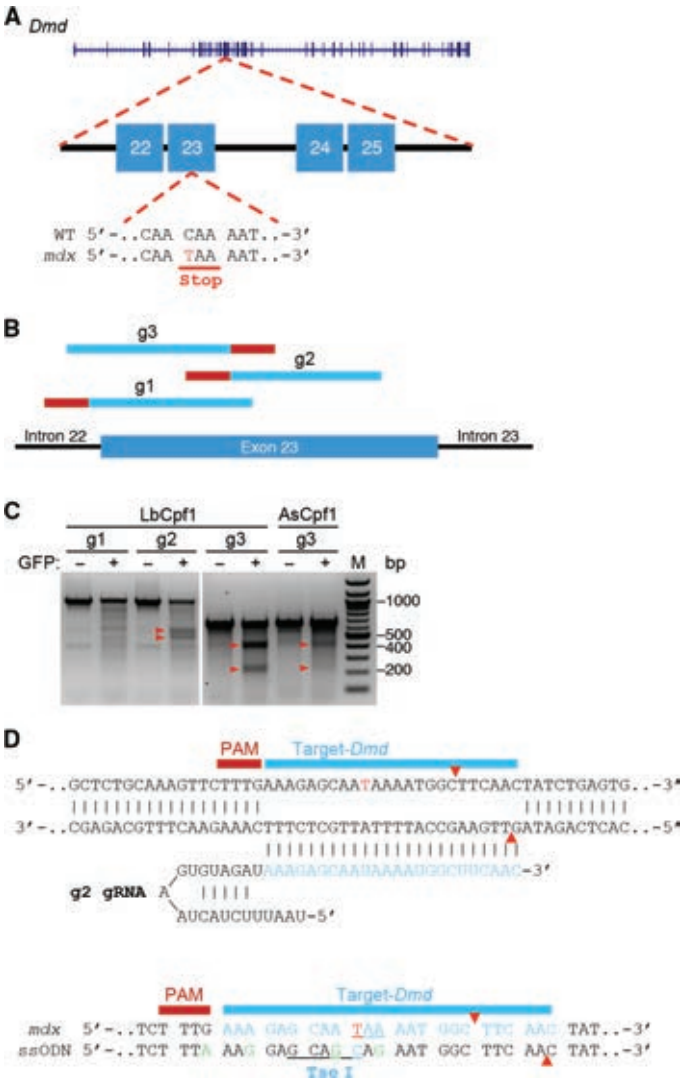

Fig. 4. CRISPR-Cpf1–mediated editing of exon 23 of the mouse *Dmd* gene. (**A**) Illustration of mouse *Dmd* locus highlighting the mutation at exon 23. Sequence shows the nonsense mutation caused by C-to-T transition, which creates a premature stop codon. (**B**) Illustration showing the targeting location of gRNAs (g1, g2, and g3) (in light blue) in exon 23 of the *Dmd* gene. Red line represents LbCpf1 PAM. (**C**) T7E1 assay using mouse 10T1/2 cells transfected with LbCpf1 or AsCpf1 with different gRNAs (g1, g2, or g3) targeting exon 23 shows that LbCpf1 and AsCpf1 have different cleavage efficiency at the *Dmd* exon 23 locus. Red arrowheads show cleavage products of genome editing. M, marker. (**D**) Illustration of LbCpf1-mediated gRNA (g2) targeting of *Dmd* exon 23. Red arrowheads indicate the cleavage site. The ssODN HDR template contains the *mdx* correction, four silent mutations (green), and a Tse I restriction site (underlined).

full restoration of dystrophin protein and displayed no sign of fibrosis or inflammatory infiltration, which is consistent with our previous study (*7*). Western blot analysis showed expression of dystrophin protein in multiple skeletal muscle groups, heart, and brain (fig. S8), consistent with percentages of dystrophin-positive fibers seen with immunohistochemistry (fig. S6).

LbCpf1-mediated correction of the *Dmd* mutation in germ cells was evaluated in eggs and sperm of LbCpf1-corrected *mdx*-C mice by T7E1 assays and Tse I RFLP. All LbCpf1-corrected *mdx*-C mice carried a corrected allele in their germ cells (fig. S9). Genome editing efficiency

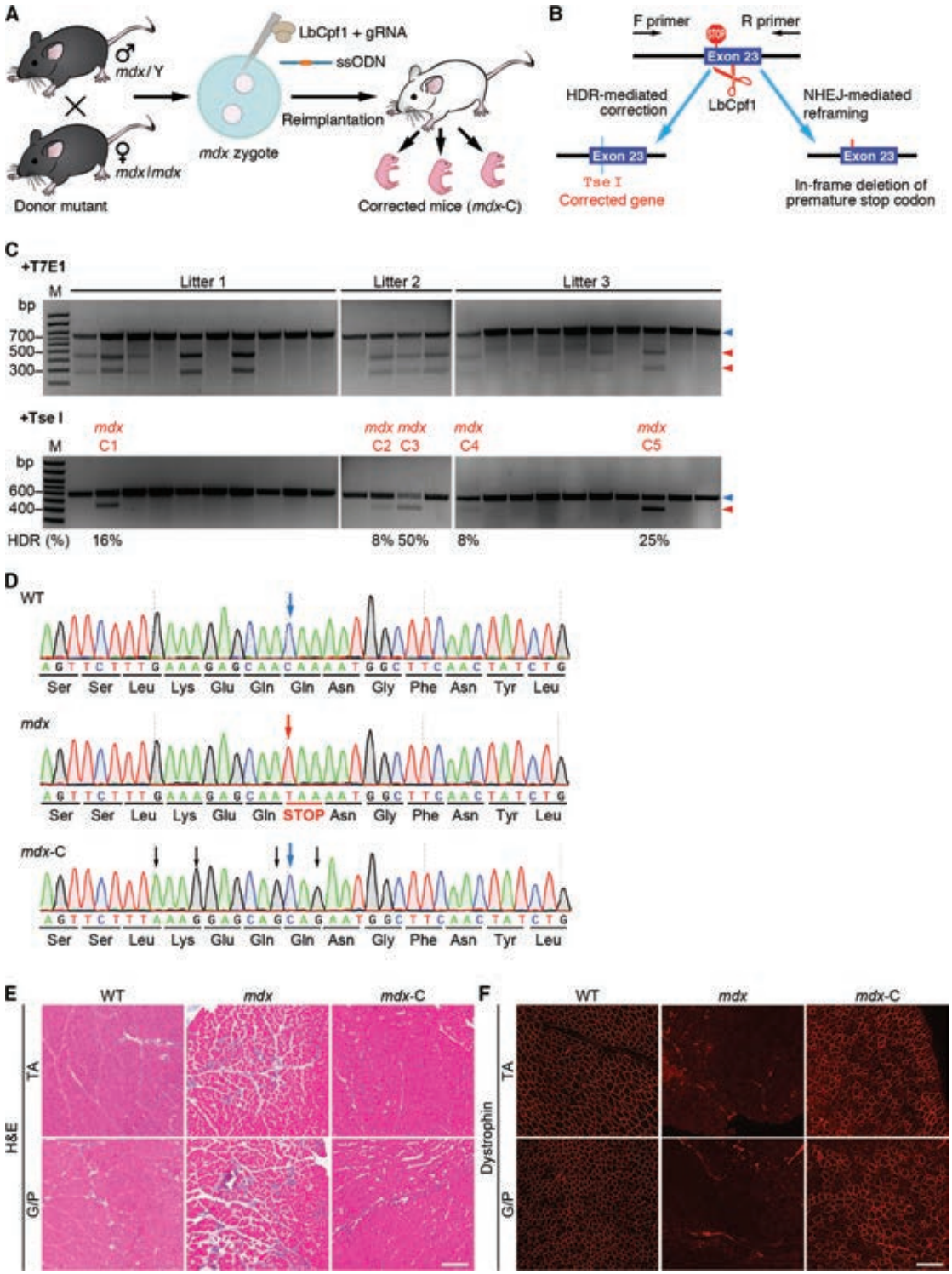

Fig. 5. CRISPR-LbCpf1–mediated *Dmd* correction in *mdx* mice. (**A**) Strategy of gene correction in *mdx* mice by LbCpf1-mediated germline editing. Zygotes from intercrosses of *mdx* parents were injected with gene editing components (LbCpf1 mRNA, g2 gRNA, and ssODN) and reimplanted into pseudopregnant mothers, which gave rise to pups with gene correction (*mdx*-C). (**B**) Illustration showing LbCpf1 correction of *mdx* allele by HDR or NHEJ. (**C**) Genotyping results of LbCpf1-edited *mdx* mice. Top: T7E1 assay. Blue arrowhead denotes uncleaved DNA, and red arrowhead shows T7E1-cleaved DNA. Bottom: Tse I RFLP assay. Blue arrowhead denotes uncorrected DNA, and red arrowhead points to Tse I cleavage, indicating HDR correction. *mdx*-C1 to *mdx*-C5 denote LbCpf1-edited *mdx* mice. (**D**) Top: Sequence of WT *Dmd* exon 23. Middle: Sequence of *mdx Dmd* exon 23 with C-to-T mutation, which generates a stop codon. Bottom: Sequence of *Dmd* exon 23 with HDR correction by LbCpf1-mediated editing. Black arrows point to silent mutations introduced by the ssODN HDR template. (**E**) H&E staining of tibialis anterior (TA) and gastrocnemius/plantaris (G/P) muscles from WT, *mdx*, and LbCpf1-edited mice (*mdx*-C). Scale bar, 100 μm. (**F**) Immunohistochemistry of tibialis anterior and gastrocnemius/plantaris muscles from WT, *mdx*, and LbCpf1-edited mice (*mdx*-C) using an antibody to dystrophin (red). *mdx* muscle showed fibrosis and inflammatory infiltration, whereas *mdx*-C muscle showed normal muscle structure.

Table 1. Serum CK measurement and forelimb grip strength of WT, *mdx*, and LbCpf1-corrected *mdx*-C mice. M, male; F, female.

Mouse no.	Percent correction by HDR	Sex	Weight (g)	CK (U/liter)	Forelimb grip strength (grams of force)						
					Trial 1	Trial 2	Trial 3	Trial 4	Trial 5	Trial 6	Average ± SD
WT-1	—	M	16.6	455	103	106	97	71	88	82	91.2 ± 13.4
WT-2	—	M	19.5	220	87	95	73	73	74	78	80.0 ± 9.1
WT-3	—	M	18.7	306	79	97	74	78	84	84	82.7 ± 8.0
WT-4	—	F	15.5	184	86	97	85	83	85	88	87.3 ± 5.0
WT-5	—	F	15.4	175	88	85	100	96	88	86	90.5 ± 6.1
WT-6	—	F	12.6	157	76	75	73	78	64	61	71.2 ± 7.0
mdx-1	0	M	18.8	8579	76	92	86	33	32	29	58.0 ± 29.9
mdx-2	0	M	21.0	9440	62	58	54	45	45	47	51.8 ± 7.3
mdx-3	0	M	21.5	5936	77	54	69	57	56	61	62.3 ± 8.9
mdx-4	0	F	16.1	6306	69	63	69	61	67	60	64.8 ± 4.0
mdx-5	0	F	15.8	6349	83	88	85	59	55	54	70.7 ± 16.2
mdx-6	0	F	16.2	4168	69	71	53	59	59	57	61.3 ± 7.1
mdx-C1	16%	F	21.7	1233	112	111	112	115	101	109	110.0 ± 4.8
mdx-C2	8%	F	19.7	4920	119	109	108	95	86	85	100.3 ± 13.8
mdx-C3	50%	F	20.2	248	110	115	114	112	112	104	111.2 ± 3.9
mdx-C4	8%	M	22.7	6607	49	45	42	30	25	21	35.3 ± 11.5
mdx-C5	25%	F	17.7	3239	92	110	96	91	110	95	99.0 ± 8.7

of Cas9 and LbCpf1 was compared at the *Dmd* exon 23 locus, and no significant difference was observed (table S3).

Physiological and functional analyses were also performed in WT, *mdx*, and LbCpf1-corrected *mdx*-C mice. Serum creatine kinase (CK) levels were decreased substantially in *mdx*-C mice and were inversely correlated with the percentage of genome correction (Table 1). The forelimb grip strength test indicated that LbCpf1-corrected *mdx*-C mice had improved muscle strength compared to *mdx* mice (Table 1).

DISCUSSION

Here, we show that the newly discovered CRISPR-Cpf1 nuclease can efficiently correct *DMD* mutations in patient-derived iPSCs and *mdx* mice, allowing for restoration of dystrophin expression. Lack of dystrophin in DMD has been shown to disrupt the integrity of the sarcolemma, causing mitochondrial dysfunction and oxidative stress (*28*, *29*). We found increased mtDNA and higher OCRs in LbCpf1-corrected iPSC-derived cardiomyocytes compared to uncorrected DMD iPSC-derived cardiomyocytes. Metabolic abnormalities of human DMD iPSC-derived cardiomyocytes were also rescued by Cpf1-mediated genomic editing. Our findings also demonstrated the robustness and efficiency of Cpf1 in mouse genome editing. By using HDR-mediated correction, the ORF of the mouse *Dmd* gene was completely restored, and pathophysiological hallmarks of the dystrophic phenotype, such as fibrosis and inflammatory infiltration, were also rescued.

Two different strategies—reframing and exon skipping—were applied to restore the ORF of the *DMD* gene using LbCpf1-mediated genome editing. Reframing creates small INDELs and restores the ORF by placing out-of-frame codons in frame. Only one gRNA is required for reframing. Although we did not observe any differences in subcellular localization between WT dystrophin protein and reframed dystrophin protein by immunocytochemistry, we observed differences in dystrophin expression level, mtDNA quantity, and OCR in different edited clones, suggesting that reframed dystrophin may not be structurally or functionally identical to WT dystrophin.

Various issues should be considered with respect to the use of one or two gRNAs with Cpf1 editing. Here, we show that two gRNAs are more effective than one gRNA for disruption of the splice acceptor site compared to reframing. When using two gRNAs, Cpf1 editing excises the intervening region and not only removes the splice acceptor site but also can be designed to remove deleterious "AG" nucleotides, eliminating the possibility of generating a pseudosplice acceptor site. However, with two gRNAs, there is the necessity that both gRNAs cleave simultaneously, which may not occur. If only one of the two gRNAs cleaves, the desired deletion will not be generated. However, there remains the possibility that cleavage with one of the two gRNAs will generate INDELS at the targeted exon region, reframing the ORF, because in theory, one-third of the INDELS will be in frame. Using one gRNA to disrupt the splice acceptor site seems more efficient because it eliminates the need for two simultaneous cuts to occur. However, there is uncertainty with respect to the length of the INDEL generated by one gRNA-mediated

editing. With one gRNA, there remains the possibility of leaving exonic AG nucleotides near the cleavage site, which can serve as an alternative pseudosplice acceptor site.

With its unique T-rich PAM sequence, Cpf1 further expands the genome editing range of the CRISPR family, which is important for potential correction of other disease-related mutations because not all mutation sites contain G-rich PAM sequences for SpCas9 or PAMs for other Cas9 orthologs. Moreover, the staggered cut generated by Cpf1 may also be advantageous for NHEJ-mediated genome editing (*30*). Finally, the LbCpf1 used in this study is 140 amino acids smaller than the most widely used SpCas9, which would enhance packaging and delivery by AAV.

Our off-target analysis by T7E1 assays and quantitative capillary electrophoresis using a fragment analyzer showed similar results to previous reports (*16*, *17*), indicating that LbCpf1 and AsCpf1 had high genome-wide targeting efficiency and high specificity comparable to those of SpCas9. This is reflective of LbCpf1 and AsCpf1 not tolerating mismatches at the 5′ PAM proximal region, thereby lessening the frequency of off-targeting effect.

Our findings show that Cpf1 is highly efficient in correcting human *DMD* and mouse *Dmd* mutations in vitro and in vivo. CRISPR-Cpf1–mediated genome editing represents a new and powerful approach to permanently eliminate genetic mutations and rescue abnormalities associated with DMD and other disorders.

MATERIALS AND METHODS

Generation of pLbCpf1-2A-GFP and pAsCpf1-2A-GFP plasmids

Human codon-optimized LbCpf1 and AsCpf1 were PCR-amplified from the pY016 plasmid (*14*) (pcDNA3.1-hLbCpf1), a gift from F. Zhang (Addgene plasmid #69988), and the pY010 plasmid (*14*) (pcDNA3.1-hAsCpf1), a gift from F. Zhang (Addgene plasmid #69982), respectively. Cpf1 complementary DNA (cDNA) and T2A-GFP DNA fragment were cloned into the backbone of the pSpCas9(BB)-2A-GFP (PX458) plasmid (*13*), a gift from F. Zhang (Addgene plasmid #48138), which was cut with Age I/Eco RI to remove SpCas9(BB)-2A-GFP. In-Fusion HD Cloning Kit (Takara Bio) was used. Cpf1 gRNAs targeting the human *DMD* or the mouse *Dmd* locus were subcloned into newly generated pLbCpf1-2A-GFP and pAsCpf1-2A-GFP plasmids using Bbs I digestion and T4 ligation. Detailed primer sequences can be found in the Supplementary Materials (table S4).

Human iPSC maintenance, nucleofection, and differentiation

Human iPSCs (RBRC-HPS0164) were purchased from Cell Bank RIKEN BioResource Center. Human iPSCs were cultured in mTeSR1 medium (STEMCELL Technologies) and passaged approximately every 4 days (1:18 split ratio). One hour before nucleofection, iPSCs were treated with 10 μM ROCK inhibitor (Y-27632) and dissociated into single cells using Accutase (Innovative Cell Technologies Inc.). iPSCs (1×10^6) were mixed with 5 μg of the pLbCpf1-2A-GFP or pAsCpf1-2A-GFP plasmid and nucleofected using the P3 Primary Cell 4D-Nucleofector X Kit (Lonza) according to the manufacturer's protocol. After nucleofection, iPSCs were cultured in mTeSR1 medium supplemented with 10 μM ROCK inhibitor, penicillin-streptomycin (1:100) (Thermo Fisher Scientific), and Primocin (100 μg/ml; InvivoGen). Three days after nucleofection, GFP(+) and GFP(−) cells were sorted by FACS and subjected to the T7E1 assay. Single clones derived from GFP(+) iPSCs were picked and sequenced. iPSCs were induced to differentiate into cardiomyocytes, as previously described (*27*).

Genomic DNA isolation

Genomic DNA of mouse 10T1/2 fibroblasts and human iPSCs was isolated using a Quick-gDNA MiniPrep kit (Zymo Research) according to the manufacturer's protocol.

Reverse transcription PCR

RNA was isolated using TRIzol (Thermo Fisher Scientific) according to the manufacturer's protocol. cDNA was synthesized using the iScript Reverse Transcription Supermix (Bio-Rad Laboratories) according to the manufacturer's protocol. RT-PCR was performed using primers flanking *DMD* exons 47 and 52 (forward, 5′-CCCAGAAGAGCAAGATAAACTTGAA-3′; reverse, 5′-CTCTGTTCCAAATCCTGCTTGT-3′). RT-PCR products amplified from WT cardiomyocytes, uncorrected cardiomyocytes, and exon 51–skipped cardiomyocytes were 712, 320, and 87 bp, respectively.

Dystrophin Western blot analysis

Western blot analysis for human iPSC-derived cardiomyocytes was performed, as previously described (*7*), using a rabbit anti-dystrophin antibody (Abcam, ab15277) and a mouse anti-cardiac myosin heavy chain antibody (Abcam, ab50967). For mouse skeletal muscles, heart, and brain, the Western blot was performed, as previously described (*7*), using a mouse anti-dystrophin antibody (Sigma-Aldrich, D8168) and a mouse anti-vinculin antibody (Sigma-Aldrich, V9131).

Dystrophin immunocytochemistry and immunohistochemistry

iPSC-derived cardiomyocytes were fixed with acetone, blocked with serum cocktail [2% normal horse serum/2% normal donkey serum/0.2% bovine serum albumin (BSA)/phosphate-buffered saline (PBS)], and incubated with a dystrophin antibody (MANDYS8, 1:800; Sigma-Aldrich) and troponin I antibody (H170, 1:200; Santa Cruz Biotechnology) in 0.2% BSA/PBS. Following overnight incubation at 4°C, they were incubated with secondary antibodies [biotinylated horse anti-mouse immunoglobulin G (IgG), 1:200 (Vector Laboratories), and fluorescein-conjugated donkey anti-rabbit IgG, 1:50 (Jackson ImmunoResearch)] for 1 hour. Nuclei were counterstained with Hoechst 33342 (Molecular Probes).

Immunohistochemistry of skeletal muscles, heart, and brain was performed, as previously described (*7*, *12*), using a dystrophin antibody (MANDYS8, 1:800; Sigma-Aldrich). Nuclei were counterstained with Hoechst 33342 (Molecular Probes).

mtDNA copy number quantification

Genomic DNA and mtDNA were isolated using TRIzol, followed by back extraction, as previously described (*31*). KAPA SYBR FAST qPCR Kit (Kapa Biosystems) was used to perform real-time PCR to quantitatively determine mtDNA copy number. Human mitochondrial *ND1* gene was amplified using primers (forward, 5′-CGCCACATCTACCATCACCCTC-3′; reverse, 5′-CGGCTAGGCTAGAGGTGGCTA-3′). Human genomic *LPL* gene was amplified using primers (forward, 5′-GAGTATGCAGAAGCCCCGAGTC-3′; reverse, 5′-TCAACATGCCCAACTGGTTTCTGG-3′). mtDNA copy number per diploid genome was calculated using the following formulas: ΔC_T = (mtND1 C_T – LPL C_T) and mtDNA copy number per diploid genome = $2 \times 2^{-\Delta CT}$.

Cellular respiration rates

OCRs were determined in human iPSC-derived cardiomyocytes using the XF24 Extracellular Flux Analyzer (Seahorse Bioscience) following the manufacturer's protocol, as previously described (*32*).

In vitro transcription of LbCpf1 mRNA and gRNA

Human codon-optimized LbCpf1 was PCR-amplified from pLbCpf1-2A-GFP to include the T7 promoter sequence (table S4). The PCR product was transcribed using the mMESSAGE mMACHINE T7 Transcription Kit (Thermo Fisher Scientific) according to the manufacturer's protocol. Synthesized LbCpf1 mRNAs were polyadenylate [poly(A)]–tailed with *E. coli* Poly(A) Polymerase (New England Biolabs) and purified using NucAway spin columns (Thermo Fisher Scientific).

The template for LbCpf1 gRNA in vitro transcription was PCR-amplified from the pLbCpf1-2A-GFP plasmid and purified using the Wizard SV Gel and PCR Clean-Up System (Promega). The LbCpf1 gRNA was synthesized using the MEGAshortscript T7 Transcription Kit (Thermo Fisher Scientific) according to the manufacturer's protocol. Synthesized LbCpf1 gRNA was purified using NucAway spin columns (Thermo Fisher Scientific).

Single-stranded oligodeoxynucleotide

ssODN was used as HDR template and synthesized by Integrated DNA Technologies as 4 nM Ultramer oligonucleotides. ssODN was mixed with LbCpf1 mRNA and gRNA directly without purification. The sequence of ssODN is as follows: 5′-TGATATGAATGAAACTCAT-CAAATATGCGTGTTAGTGTAAATGAACTTCTATTTAATTTT-GAGGCTCTGCAAAGTTCTTTAAAGGAGCAGCAGAATGGCTT-CAACTATCTGAGTGACACTGTGAAGGAGATGGCCAAGAAAG-CACCTTCAGAAATATGCCAGAAATATCTGTCAGAATTT-3′.

CRISPR-Cpf1–mediated genome editing by one-cell embryo injection

All animal procedures were approved by the Institutional Animal Care and Use Committee at the University of Texas Southwestern Medical Center. Detailed injection procedures were performed as described previously (*7*). The only modification was replacing Cas9 mRNA and Cas9 gRNAs with LbCpf1 mRNA and LbCpf1 gRNAs, respectively.

PCR amplification of genomic DNA, T7E1 assay, and Tse I RFLP analysis

All these protocols were preformed as previously published (*7*).

Mouse forelimb grip strength test and serum CK measurement

Grip strength test and serum CK measurement were performed, as previously described (*7*), by the Neuro-Models Core Facility and the Metabolic Phenotyping Core at the University of Texas Southwestern Medical Center, respectively.

Off-target site analysis

Off-target sites were predicted using Cas-OFFinder (www.rgenome.net/cas-offinder/), and off-target analysis was performed as previously described (*12*). Sequences are provided in the Supplementary Materials (tables S1 and S2). For capillary electrophoresis, PCR products from control and treated samples were denatured and reannealed to form heteroduplex. T7E1-digested DNA samples were visualized by the Fragment Analyzer (Advanced Analytical), which allowed a sensitive, accurate, and fast quantification of percent cleavage. The PCR sample (2 μl) was diluted with the sample buffer (DNF-910-1000CP CRISPR kit) and loaded into the 96-well sample plate. Cleavage percentage was calculated by CRISPR Plugin for PROSize 2.0. Expected full-length and cleavage fragment sizes of PCR samples were entered into the software. Highlighted fragments with automated scores were shown in figs. S3B and S4B. Concentration of each peak and percentage cleavage value were automatically calculated by the software. Reconstructed gel images from the Fragment Analyzer electropherogram were shown in figs. S3A and S4A.

Statistical analysis

Statistical analysis was assessed by two-tailed Student's *t* test. Data are shown as means ± SEM. A $P < 0.05$ value was considered statistically significant.

SUPPLEMENTARY MATERIALS

Supplementary material for this article is available at http://advances.sciencemag.org/cgi/content/full/3/4/e1602814/DC1

fig. S1. Genome editing of *DMD* exon 51 and *Dmd* exon 23 by LbCpf1 or AsCpf1.
fig. S2. Genomic PCR and T7E1 assay of off-target sites.
fig. S3. Capillary electrophoresis and fragment analysis of *DMD* g1 off-target sites.
fig. S4. Capillary electrophoresis and fragment analysis of *DMD* g2 off-target sites.
fig. S5. Histological analysis of muscles from WT, *mdx*, and LbCpf1-edited mice (*mdx*-C).
fig. S6. Immunohistochemistry of skeletal muscles, heart, and brain from WT, *mdx*, and LbCpf1-edited mice (*mdx*-C).
fig. S7. H&E staining of skeletal muscles, heart, and brain from WT, *mdx*, and LbCpf1-edited mice (*mdx*-C).
fig. S8. Western blot analysis of skeletal muscles, heart, and brain from WT, *mdx*, and LbCpf1-edited mice (*mdx*-C).
fig. S9. T7E1 and Tse I RFLP analysis of germ cells from LbCpf1-edited mice (*mdx*-C) and uncorrected *mdx* mice.
table S1. Sequence of the on-target site and 10 potential off-target sites.
table S2. Primers used in the off-target site analysis.
table S3. Comparison of CRISPR-Cas9– and CRISPR-Cpf1–mediated HDR correction in *mdx* mice.
table S4. Sequence of primers.

REFERENCES AND NOTES

1. K. P. Campbell, S. D. Kahl, Association of dystrophin and an integral membrane glycoprotein. *Nature* **338**, 259–262 (1989).
2. K. Hollinger, J. S. Chamberlain, Viral vector-mediated gene therapies. *Curr. Opin. Neurol.* **28**, 522–527 (2015).
3. B. Bostick, J.-H. Shin, Y. Yue, D. Duan, AAV-microdystrophin therapy improves cardiac performance in aged female *mdx* mice. *Mol. Ther.* **19**, 1826–1832 (2011).
4. Y. Shimizu-Motohashi, S. Miyatake, H. Komaki, S. Takeda, Y. Aoki, Recent advances in innovative therapeutic approaches for Duchenne muscular dystrophy: From discovery to clinical trials. *Am. J. Transl. Res.* **8**, 2471–2489 (2016).
5. F. J. M. Mojica, C. Díez-Villaseñor, J. García-Martínez, E. Soria, Intervening sequences of regularly spaced prokaryotic repeats derive from foreign genetic elements. *J. Mol. Evol.* **60**, 174–182 (2005).
6. Y. Wu, D. Liang, Y. Wang, M. Bai, W. Tang, S. Bao, Z. Yan, D. Li, J. Li, Correction of a genetic disease in mouse via use of CRISPR-Cas9. *Cell Stem Cell* **13**, 659–662 (2013).
7. C. Long, J. R. McAnally, J. M. Shelton, A. A. Mireault, R. Bassel-Duby, E. N. Olson, Prevention of muscular dystrophy in mice by CRISPR/Cas9–mediated editing of germline DNA. *Science* **345**, 1184–1188 (2014).
8. H. Yin, W. Xue, S. Chen, R. L. Bogorad, E. Benedetti, M. Grompe, V. Koteliansky, P. A. Sharp, T. Jacks, D. G. Anderson, Genome editing with Cas9 in adult mice corrects a disease mutation and phenotype. *Nat. Biotechnol.* **32**, 551–553 (2014).
9. M. Tabebordbar, K. Zhu, J. K. W. Cheng, W. L. Chew, J. J. Widrick, W. X. Yan, C. Maesner, E. Y. Wu, R. Xiao, F. A. Ran, L. Cong, F. Zhang, L. H. Vandenberghe, G. M. Church, A. J. Wagers, In vivo gene editing in dystrophic mouse muscle and muscle stem cells. *Science* **351**, 407–411 (2016).
10. C. E. Nelson, C. H. Hakim, D. G. Ousterout, P. I. Thakore, E. A. Moreb, R. M. Castellanos Rivera, S. Madhavan, X. Pan, F. A. Ran, W. X. Yan, A. Asokan, F. Zhang, D. Duan, C. A. Gersbach, In vivo genome editing improves muscle function in a mouse model of Duchenne muscular dystrophy. *Science* **351**, 403–407 (2016).

11. M. A. DeWitt, W. Magis, N. L. Bray, T. Wang, J. R. Berman, F. Urbinati, S.-J. Heo, T. Mitros, D. P. Muñoz, D. Boffelli, D. B. Kohn, M. C. Walters, D. Carroll, D. I. K. Martin, J. E. Corn, Selection-free genome editing of the sickle mutation in human adult hematopoietic stem/progenitor cells. *Sci. Transl. Med.* **8**, 360ra134 (2016).
12. C. Long, L. Amoasii, R. Bassel-Duby, E. N. Olson, Genome editing of monogenic neuromuscular diseases: A systematic review. *JAMA Neurol.* **73**, 1349–1355 (2016).
13. F. A. Ran, L. Cong, W. X. Yan, D. A. Scott, J. S. Gootenberg, A. J. Kriz, B. Zetsche, O. Shalem, X. Wu, K. S. Makarova, E. V. Koonin, P. A. Sharp, F. Zhang, In vivo genome editing using *Staphylococcus aureus* Cas9. *Nature* **520**, 186–191 (2015).
14. B. Zetsche, J. S. Gootenberg, O. O. Abudayyeh, I. M. Slaymaker, K. S. Makarova, P. Essletzbichler, S. E. Volz, J. Joung, J. van der Oost, A. Regev, E. V. Koonin, F. Zhang, Cpf1 is a single RNA-guided endonuclease of a class 2 CRISPR-Cas system. *Cell* **163**, 759–771 (2015).
15. Y. Kim, S.-A. Cheong, J. G. Lee, S.-W. Lee, M. S. Lee, I.-J. Baek, Y. H. Sung, Generation of knockout mice by Cpf1-mediated gene targeting. *Nat. Biotechnol.* **34**, 808–810 (2016).
16. D. Kim, J. Kim, J. K. Hur, K. W. Been, S.-h. Yoon, J.-S. Kim, Genome-wide analysis reveals specificities of Cpf1 endonucleases in human cells. *Nat. Biotechnol.* **34**, 876–881 (2016).
17. S. Q. Tsai, M. S. Prew, N. T. Nguyen, M. M. Welch, J. M. Lopez, Z. R. McCaw, M. J. Aryee, B. P. Kleinstiver, J. K. Joung, Genome-wide specificities of CRISPR-Cas Cpf1 nucleases in human cells. *Nat. Biotechnol.* **34**, 882–887 (2016).
18. E. Tóth, N. Weinhardt, P. Bencsura, K. Huszár, P. I. Kulcsár, A. Tálas, E. Fodor, E. Welker, Cpf1 nucleases demonstrate robust activity to induce DNA modification by exploiting homology directed repair pathways in mammalian cells. *Biol. Direct* **11**, 46 (2016).
19. M. Jinek, K. Chylinski, I. Fonfara, M. Hauer, J. A. Doudna, E. Charpentier, A programmable dual-RNA–guided DNA endonuclease in adaptive bacterial immunity. *Science* **337**, 816–821 (2012).
20. I. Fonfara, H. Richter, M. Bratovič, A. Le Rhun, E. Charpentier, The CRISPR-associated DNA-cleaving enzyme Cpf1 also processes precursor CRISPR RNA. *Nature* **532**, 517–521 (2016).
21. C. Long, L. Amoasii, A. A. Mireault, J. R. McAnally, H. Li, E. Sanchez-Ortiz, S. Bhattacharyya, J. M. Shelton, R. Bassel-Duby, E. N. Olson, Postnatal genome editing partially restores dystrophin expression in a mouse model of muscular dystrophy. *Science* **351**, 400–403 (2016).
22. C. S. Young, M. R. Hicks, N. V. Ermolova, H. Nakano, M. Jan, S. Younesi, S. Karumbayaram, C. Kumagai-Cresse, D. Wang, J. A. Zack, D. B. Kohn, A. Nakano, S. F. Nelson, M. C. Miceli, M. J. Spencer, A. D. Pyle, A single CRISPR-Cas9 deletion strategy that targets the majority of DMD patients restores dystrophin function in hiPSC-derived muscle cells. *Cell Stem Cell* **18**, 533–540 (2016).
23. L. Xu, K. H. Park, L. Zhao, J. Xu, M. El Refaey, Y. Gao, H. Zhu, J. Ma, R. Han, CRISPR-mediated genome editing restores dystrophin expression and function in *mdx* mice. *Mol. Ther.* **24**, 564–569 (2016).
24. A. Aartsma-Rus, I. Fokkema, J. Verschuuren, I. Ginjaar, J. van Deutekom, G.-J. van Ommen, J. T. den Dunnen, Theoretic applicability of antisense-mediated exon skipping for Duchenne muscular dystrophy mutations. *Hum. Mutat.* **30**, 293–299 (2009).
25. S. Cirak, V. Arechavala-Gomeza, M. Guglieri, L. Feng, S. Torelli, K. Anthony, S. Abbs, M. E. Garralda, J. Bourke, D. J. Wells, G. Dickson, M. J. Wood, S. D. Wilton, V. Straub, R. Kole, S. B. Shrewsbury, C. Sewry, J. E. Morgan, K. Bushby, F. Muntoni, Exon skipping and dystrophin restoration in patients with Duchenne muscular dystrophy after systemic phosphorodiamidate morpholino oligomer treatment: An open-label, phase 2, dose-escalation study. *Lancet* **378**, 595–605 (2011).
26. R. A. Padgett, New connections between splicing and human disease. *Trends Genet.* **28**, 147–154 (2012).
27. P. W. Burridge, E. Matsa, P. Shukla, Z. C. Lin, J. M. Churko, A. D. Ebert, F. Lan, S. Diecke, B. Huber, N. M. Mordwinkin, J. R. Plews, O. J. Abilez, B. Cui, J. D. Gold, J. C. Wu, Chemically defined generation of human cardiomyocytes. *Nat. Methods* **11**, 855–860 (2014).
28. D. P. Millay, M. A. Sargent, H. Osinska, C. P. Baines, E. R. Barton, G. Vuagniaux, H. L. Sweeney, J. Robbins, J. D. Molkentin, Genetic and pharmacologic inhibition of mitochondrial-dependent necrosis attenuates muscular dystrophy. *Nat. Med.* **14**, 442–447 (2008).
29. F. Mourkioti, J. Kustan, P. Kraft, J. W. Day, M.-M. Zhao, M. Kost-Alimova, A. Protopopov, R. A. DePinho, D. Bernstein, A. K. Meeker, H. M. Blau, Role of telomere dysfunction in cardiac failure in Duchenne muscular dystrophy. *Nat. Cell Biol.* **15**, 895–904 (2013).
30. M. Maresca, V. G. Lin, N. Guo, Y. Yang, Obligate ligation-gated recombination (ObLiGaRe): Custom-designed nuclease-mediated targeted integration through nonhomologous end joining. *Genome Res.* **23**, 539–546 (2013).
31. C. Zechner, L. Lai, J. F. Zechner, T. Geng, Z. Yan, J. W. Rumsey, D. Collia, Z. Chen, D. F. Wozniak, T. C. Leone, D. P. Kelly, Total skeletal muscle PGC-1 deficiency uncouples mitochondrial derangements from fiber type determination and insulin sensitivity. *Cell Metab.* **12**, 633–642 (2010).
32. K. K. Baskin, C. E. Grueter, C. M. Kusminski, W. L. Holland, A. L. Bookout, S. Satapati, Y. M. Kong, S. C. Burgess, C. R. Malloy, P. E. Scherer, C. B. Newgard, R. Bassel-Duby, E. N. Olson, MED13-dependent signaling from the heart confers leanness by enhancing metabolism in adipose tissue and liver. *EMBO Mol. Med.* **6**, 1610–1621 (2014).

Acknowledgments: We thank J. Cabrera for assistance with graphics. **Funding:** This work was supported by grants from the NIH (HL130253, HL-077439, DK-099653, and AR-067294), a Paul D. Wellstone Muscular Dystrophy Cooperative Research Center grant (U54 HD 087351), and the Robert A. Welch Foundation (grant 1-0025 to E.N.O.). **Author contributions:** Y.Z., C.L., and E.N.O. designed the project; Y.Z., H.L., J.R.M., K.K.B., and J.M.S. performed the experiments; Y.Z., C.L., R.B.-D., and E.N.O. wrote and edited the manuscript. **Competing interests:** R.B.-D. and E.N.O. are consultants for Exonics Therapeutics. E.N.O., Y.Z., C.L., and R.B.-D. are listed on the patent entitled "Prevention of muscular dystrophy by CRISPR/Cpf1-mediated gene editing" (U.S. Patent 62/426,853, 28 November 2016). The other authors declare that they have no competing interests. **Data and materials availability:** All data needed to evaluate the conclusions in the paper are present in the paper and/or the Supplementary Materials. Additional data related to this paper may be requested from the authors.

Submitted 13 November 2016
Accepted 14 February 2017
Published 12 April 2017
10.1126/sciadv.1602814

Citation: Y. Zhang, C. Long, H. Li, J. R. McAnally, K. K. Baskin, J. M. Shelton, R. Bassel-Duby, E. N. Olson, CRISPR-Cpf1 correction of muscular dystrophy mutations in human cardiomyocytes and mice. *Sci. Adv.* **3**, e1602814 (2017).